Photosynthetic capacity and assimilate transport of the lower canopy influence maize yield under high planting density

Yanyan Yan[1, 3], Fengying Duan[1,2], Xia Li[1,2], Rulang Zhao[4], Peng Hou[1], Ming Zhao[1], Shaokun Li[1], Yonghong Wang[4], Tingbo Dai[3], Wenbin Zhou[1,2]*

[1] Institute of Crop Sciences, Chinese Academy of Agricultural Sciences, Beijing 100081, China

[2] State Key Laboratory of Crop Gene Resources and Breeding, Institute of Crop Sciences, Chinese Academy of Agricultural Sciences, Beijing 100081, China

[3] Key Laboratory of Crop Physiology Ecology and Production Management of Ministry of Agriculture, Nanjing Agricultural University, Nanjing 210095, China

[4] Ningxia Academy of Agriculture and Forestry Sciences, Crops Research Institute, Yinchuan 750105, China

* Corresponding author:

Tel: +86 10 82107841; Email address: zhouwenbin@caas.cn (Wenbin Zhou)

Short title: Maize grain yield under high planting density

The author responsible for distribution of materials integral to the findings presented in this article in accordance with the policy described in the Instructions for Authors (https://academic.oup.com/plphys/pages/General-Instructions) is Wenbin Zhou (zhouwenbin@caas.cn).

Abstract

Photosynthesis is a major trait of interest for development of high-yield crop plants. However, little is known about the effects of high-density planting on photosynthetic responses at the whole-canopy level. Using the high-yielding maize (*Zea mays* L.) cultivars 'LY66', 'MC670', and 'JK968', we here conducted a two-year field experiment to assess ear development in addition to leaf characteristics and photosynthetic parameters in each canopy layer at four planting densities. Increased planting density promoted high grain yield and population-scale biomass accumulation despite reduced per-plant productivity. MC670 had the strongest adaptability to high-density planting conditions. Physiological analysis showed that increased planting density primarily led to decreases in the single-leaf area above the ear for LY66 and MC670 and below the ear for JK968. Furthermore, high planting density decreased chlorophyll content and the photosynthetic rate due to decreased canopy transmission, leading to severe decreases in single-plant biomass accumulation in the lower canopy. Moreover, increased planting density improved pre-silking biomass transfer, especially in the lower canopy. Yield showed significant positive relationships with photosynthesis and biomass in the lower canopy, demonstrating the important contributions of these leaves to grain yield under dense planting conditions. Increased planting density led to retarded ear development as a consequence of reduced glucose and fructose contents in the ears, indicating reductions in sugar transport that were associated with limited sink organ development, reduced kernel number, and yield loss. Overall, these findings highlighted the photosynthetic capacities of the lower canopy as promising targets for improving maize yield under dense planting conditions.

Keywords: maize; planting density; photosynthesis; biomass accumulation; ear development; grain yield

Introduction

To meet the nutritional demands of the 9 billion humans who are predicted to live on earth by 2050, a 60–100% increase in crop production is necessary (Prajal et al., 2015; Tian et al., 2021). Target species for increased production include grains such as maize (*Zea mays* L.), which is a staple food throughout the world and is currently the most abundantly produced of all cereal crops (FAO, 2021). As the second-largest maize producer, China contributes 23% of the global maize supply and contains 21% of the maize-growing area (FAO, 2021). However, rapid urbanization, the economic growth and growing domestic meat consumption over the past two decades has led to a widespread increasing occupation and fragmentation of arable land, including maize-growing land (Zhang et al., 2023; Xin et al., 2023). In the face of limited available arable land for maize growth, it is crucial to improve maize production per unit area to ensure food security.

Planting density is one of the most important agronomic practices in maize production (Zheng et al., 2017; Luo et al., 2023). Increasing planting density has been shown to improve maize yield by an average of 17–20% (Assefa et al., 2018). This approach can allow optimal use of available sunlight, promoting efficient conversion of carbon dioxide and water into maize grains (Ma et al., 2020; Simkin et al., 2019; Hu et al., 2020). However, dense planting can lead to intra-specific competition for available resources, namely light (in the aerial tissues) and nutrients and water (in the roots) (Deng et al., 2012; Duan et al., 2023). This can result in decreased per-plant growth and yield (Yan et al., 2021), although the effects vary significantly between maize varieties.

At the whole-field scale, vertical light interception and light absorption in specific canopy layers are strongly affected by the canopy architecture (Sarlikioti et al., 2011; Sultana et al., 2023). Previous studies have shown that variability in the light environment along the vertical canopy profile significantly impacts leaf physiology, energy dissipation, and photosynthetic capacity (Andrea et al., 2016). Therefore, photoassimilation (and subsequently yield) in each layer along the canopy profile are directly dependent on canopy architecture. Several studies have indicated that intermediate or upper leaves in the canopy contribute a majority of maize carbon accumulation and grain yield (Allison and Watson 1966; Xu et al., 2021; Slattery et al., 2018). However, overall canopy productivity is still significantly affected by the lower layers. Increased planting density reduces light penetration into these layers

(Timlin et al., 2014); plant shade responses thus strongly influence yield production under high planting density conditions. Decreased light availability can accelerate senescence and decreases radiation utilization efficiency, thus reducing per-plant yield (Zhang et al., 2019; Guo et al., 2021). Despite these prior findings, a systematic understanding of the relationship between canopy structure and maize grain yield remains lacking.

Maize is a cross-pollination crop with two distinct inflorescences, referred to as the tassel (male) and the ear (female). These structures share common developmental processes in their early stages but have unique structural features at maturity that directly affect yield (Parvathaneni et al., 2020). Maize genotype is the primary determinant controlling ear and tassel development (Wilson et al., 1978). However, crop management strategies and environmental factors, such as planting density, drought, shading, and soil fertility, also lead to variations in ear/tassel differentiation (Zhang et al., 2009; Hu et al., 2022). Previous studies have indicated that intra-specific competition for nutrients, water, and light can severely affect kernel number per ear and tassel size in maize planted at high density (Pagano et al., 2007; Zhang et al., 2018). Additionally, the extended anthesis–silking interval (ASI) induced by high density causes asynchronous flowering, hindering successful pollination and leading to yield losses of ~40–50% (Uribelarrea et al., 2008; Sher et al., 2017). Thus, ASI is a critical trait contributing to density tolerance in maize, although the physiological mechanism underlying ASI-associated yield loss under high-density planting is largely unclear.

To delineate the mechanisms associated with maize single-plant yield loss under high-density planting conditions, we here conducted a two-year field experiment in the high-yield maize ecosystem of northwestern China. Systematic analyses were carried out to characterize physiological changes in three high-yielding maize varieties grown at four planting densities. The response patterns of photosynthetic- and yield-related traits along the canopy layers were measured and differences in the effects of planting density on ear and tassel development were assessed. This approach was designed to comprehensively reveal the regulatory mechanism(s) underlying planting density responses in three maize varieties, providing key insights into density tolerance traits to ultimately promote high-yield maize breeding.

Results

Effects of planting density on maize yield and population-scale biomass accumulation in the field

The two-year field experiments were conducted in Ningxia, China during the growing seasons of 2019 and 2020 (Supplementary Fig. S1) to test the effects of planting density on yield (Table 1). Three maize varieties were planted at four densities: 75,000, 105,000, 120,000, and 135,000 plants/ha (D1–D4, respectively), and aerial plant tissues were vertically divided into four layers (layer I–IV) based on the ear position for canopy profiling (Supplementary Fig. S2). Population-scale maize yield was significantly affected by both planting density and variety, but not by the interaction between density and genotype (Table 2). As the density increased, yield tended to first increase, then decrease; and the yield peaked in the D2 group. LY66, MC670, and JK968 showed yield increases of 1.81–14.28%, 3.73–17.39%, and -3.83–8.37%, respectively, from D1 to D4 among 2-year experiments. The lower maximum yield of JK968 at high density may resulted from severe lodging, which occurred in this variety at the vegetative stage. The optimal densities of LY66, MC670, and JK968 were calculated as 10.50×10^4, 10.64×10^4, and 9.93×10^4 plants/ha, respectively; these densities corresponded to maximum yields of 19.48, 20.75, and 17.7 t/ha, respectively (Supplementary Fig. S3).

Analysis of yield components indicated that increases in yield under high-density conditions were primarily due to increases in ear number per unit area. This increase counteracted the significant decreases in kernel number per plant and 1000-kernel weight. Accordingly, high planting density resulted in significant per-plant yield decreases, especially for JK968. The barren stalk rate also increased along with the planting density, with the highest rate in JK968, followed by LY66, then MC670. Population biomass accumulation at maturity showed a similar tendency, with average increases (mean values of D2/D3/D4 – D1, among 2-year experiments) of 15.18%, 19.29%, and 5.89% in LY66, MC670, and JK968, respectively. Furthermore, increased planting density mainly caused significant biomass increases in layer II, with average increases (mean values of D2/D3/D4 – D1, among 2-year experiments) of 15.51%, 22.30% and 4.42% in LY66, MC670, and JK968, respectively (Supplementary Fig. S4). However, the harvest index (HI) decreased with planting density.

Effects of planting density on per-plant biomass accumulation and transfer in each canopy layer

We next compared per-plant biomass accumulation between specific layers of the canopy. Biomass accumulation was most abundant in layer II, followed by layer I. Increases in planting density caused pronounced decreases in per-plant biomass accumulation; across cultivars and planting years, the average decreases (mean values of D2/D3/D4 – D1) were 18.20% and 24.31% in layers I and II, respectively, at the silking stage and 35.17% and 26.92%, respectively, at the maturity stage (Fig. 1). Reductions in biomass accumulation in layers I and II were greatest in JK968, followed by LY66, then MC670. Increasing the planting density also increased the total biomass transfer, with greater positive effects observed in layers I and II (averaging 11.36 g and 3.95 g, respectively) than in layers III and IV (1.44 g and -0.04 g, respectively) (Fig. 2). Overall, biomass transfer was greatest in MC670 and lowest in LY66. These findings suggested that biomass accumulation and transport in the lower canopy were of great importance to yield formation under high-density planting conditions.

Effects of planting density on photosynthetic characteristics in each canopy layer

For individual leaves, the total area is an important indicator of photosynthetic capacity. We therefore compared the single-leaf area at each leaf position in maize plants grown at each planting density. The leaf area increased gradually with leaf position in the lower portion of the plant, peaked in the middle of the plant, then gradually decreased with leaf position in the upper plant (Fig. 3). LY66 and MC670 plants showed similar patterns of vertical leaf area distribution across planting densities. For example, LY66 and MC670 showed significant reductions in leaf area in layers III and IV as the planting density increased; in JK968, reductions in leaf area occurred instead in layers I and II (Fig. 3, Supplementary Fig. S5). Further analyze the average leaf length and average leaf width in each layer, in layers I and II, LY66 and MC670 showed increment in leaf length and slight reduction leaf width; in layers III and IV, LY66 and MC670 showed reduction in leaf length and great reduction leaf width. However, JK968 showed the opposite trend with these two varieties (Supplementary Table S1). Furthermore, the spatial density of leaf area (SDLA) generally increased with the layer number in all three varieties under high planting density. The greatest increases in layer III were found in JK968 plants

(Supplementary Fig. S6). These increases were associated with decreased fractional interception of photosynthetically active radiation (FIPAR) in layer II among JK968 plants (Supplementary Fig. S7A) and indicated poor light transmission from the top to the bottom of the plant canopy (Supplementary Fig. S7B). In addition, the red to far-red ratio (R/FR) was significantly decreased in layers I–III of LY66 and JK968 plants, but not in layers I–II of MC670 plants (Supplementary Fig. S7C). Thus, the light quality was superior in the lower canopy layers of MC670 compared to LY66 or JK968.

As a consequence of low light interception and its negative effects on leaf area, increasing the planting density significantly reduced the net photosynthetic rate (P_n) of leaves in layers I and II but not in layers III or IV (Fig. 4). Moreover, high planting density led to a greater P_n reduction among leaves in layer I (mean = 32.47%) than in layer II (mean = 19.71%). A similar trend was observed for the total chlorophyll content (Fig. 5), which increased in layer II compared to layer I, peaked in layer III, then decreased again in layer IV. The decreased of P_n and total chlorophyll contents of MC670 were reduced by a smaller margin in the lower canopy layers compared to the other varieties.

Effects of planting density on maize ear development

The maize ear length, diameter, and bald tip length were measured for each variety and treatment group at maturity. The ear length and diameter decreased along with planting density, whereas the bald tip length increased. JK968 was the most sensitive to increased planting density with respect to the increase of bald tip length (Supplementary Fig. S8). Furthermore, assessment of tassel and ear developmental processes indicated that increased planting density resulted in plant growth delays. Specifically, the silking stage was delayed by 2–3 d, 3–6 d, and 3–8 d in the D2–D4 treatments, respectively, compared to D1. However, planting density had a smaller effect at the tassel stage than at the silking stage, leading to a longer ASI among plants grown under high-density conditions (Supplementary Table S2).

Increased planting density did not appear to affect tassel development or initial ear differentiation (Fig. 6, Supplementary Fig. S9), although ear development (as measured by ear length) lagged significantly in D4 compared to D1 (Fig. 6). Stagnation in ear development under dense planting conditions was more severe as the ears grew; ear lengths in the D4 treatment were decreased by 23.77–35.09%

compared to D1 at 69 d after sowing (DAS), but by 23.18–43.67% at 77 DAS (Fig. 6). Furthermore, starch content decreased over time, whereas sucrose, glucose, and fructose contents increased as the ears grew. Starch content was significantly higher under D4 than under D1 conditions, especially at 77 DAS. Levels of glucose and fructose in the ear were significantly decreased (by 15.57–36.86% and 11.79–48.95%, respectively) in D4 compared to D1 plants (Fig. 7). Overall, ear length, glucose levels, and fructose levels were most strongly impacted by planting density in JK968 plants, followed by MC670, then LY66.

Relationships of grain yield to photosynthetic parameters at each planting density

Correlation analyses were conducted to comprehensively investigate the relationships between grain yield and physiological parameters associated with biomass accumulation and photosynthesis at each planting density (Fig. 8, Fig. S4, Fig. S8, Supplementary Dataset S1). Grain yield was positively correlated with kernel number (Fig. 8A). Moreover, kernel number was significantly correlated with ear length, ear diameter, and bald tip length (Supplementary Fig. S8, G to I). Population-scale biomass accumulation was positively correlated with grain yield (Fig. 8B), and population-scale biomass accumulation in layer I and II were positively correlated with grain yield (Supplementary Fig. S4F). Furthermore, per-plant biomass accumulation in layers I and II were positively correlated with grain weight per plant (Fig. 8, C and D), and biomass transfer in layers I and II were negatively correlated with grain weight per plant (Fig. 8E). FIPAR in layer III was negatively correlated with grain weight per plant (Fig. 8F), and P_n in layers I and II were positively correlated with grain weight per plant (Fig. 8G) and biomass accumulation per plant at maturity in layers I and II (Fig. 8, H and I). Total chlorophyll content in layer II was positively correlated with grain weight per plant (Fig. 8J). Overall, grain yield and per-plant grain yield were dependent of photosynthetic parameters in layers I and II.

Discussion

Substantial increases in maize yield have been achieved in recent decades due to advances in agricultural technologies and breeding approaches. Increasing the planting density is one of the most important crop management strategies identified for increasing maize yield (Sher et al., 2017; Zhang et al., 2020). This was clearly demonstrated in 87 farm experiments undertaken in China from 2017–2020, which showed yield gains of 7.3% due in response to increased planting density (Luo et al., 2023). However, yield increases associated with high planting density are not infinite; each variety performs best at an optimal density, beyond which yield declines (Deng et al., 2012; Mastrodomenico et al., 2018; Wei et al., 2020). In the present study, total yield was generally increased by dense planting conditions, peaking at D2 for each variety (Table 1). Yield increases in response to high planting density were greatest in MC670, followed by LY66, then JK968. These high yields resulted from the combined effects of increases in the total ear number, kernel number, and 1000-kernel weight.

Photoassimilation is the foundational basis of plant productivity and biomass production (Gaju et al., 2016), with leaves serving as the primary organs responsible for light interception and photosynthesis (Chen et al., 2019). We here found that increases in the planting density decreased the light interception area, primarily in layer II or III (Supplementary Fig. S5), and increased the SDLA (Supplementary Fig. S6). These changes reduced the photosynthetic rate and thus biomass production (Fig. 1). However, population biomass accumulation at maturity showed increases of varying degrees along with the density (Table 1, Supplementary Fig. S4). Biomass accumulation varied between varieties, but was generally highest in MC670 and lowest in JK968. Notably, biomass accumulation at both the population and single-plant scale, especially in lower canopy was positively correlated with grain yield and grain weight per plant (Fig. 8, Supplementary Fig. S4F). A recent study demonstrated that the proportion of dry matter accumulation after silking increases, whereas the dry matter transfer rate decreases, in high-yield maize (Liu et al., 2023). Here, we found that biomass accumulation after silking was decreased, but that biomass transfer was increased; this was especially true in MC670 in 2020, which showed relatively higher biomass transfer at the bottom layer (Fig. 2). We therefore propose that the strong biomass accumulation and biomass redistribution capacity of maize plants at high density, particularly below the ear, can maintain high plant productivity.

Under dense planting conditions, the spatial distribution of the leaf area is known to affect light interception and utilization (Perez et al., 2019); the altered light environment of the lower canopy (i.e., reduced light intensity and/or altered spectral composition), rather than normal aging, causes decreased efficiency among shaded leaves (Collison et al., 2020). We here observed that increased planting density generally increased the SDLA in all four canopy layers (Supplementary Fig. S6), implying that there was weaker canopy transmission and poor light quality under high-density conditions (Supplementary Fig. S7, B and C). Moreover, increased planting density reduced the per-leaf area in layers II and III (LY66 and MC670) or layers I and II (JK968) (Fig. 3, Supplementary Fig. S5). This distribution of leaf area ultimately led to great increases in SDLA within layer III of JK968 plants, contributing to higher and lower FIPAR values in layers III and II, respectively (Supplementary Fig. S7A). Furthermore, the observed leaf area patterns allowed more photosynthetically active radiation (PAR) to reach the lower layers in LY66 and MC670, resulting in higher photosynthetic rates and increased chlorophyll contents in layers I and II of these plants than in JK968 (Fig. 4, Fig. 5); those photosynthetic parameters were significantly positively correlated with per-plant yield (Fig. 8).

Numerous prior publications have focused on changes in physiological function along the vertical gradient within a canopy (Ciampitti and Vyn, 2013; Chen et al., 2015; Song et al., 2018; Odorico et al., 2019; Xu et al., 2021). Such studies have generally shown that traits related to photosynthetic capacity remain high in middle-canopy leaves, such as the ear leaf and adjacent leaves (Escobar-Gutiérrez and Combe, 2012; Song et al., 2018; Xu et al., 2021). We here found that chlorophyll content was highest in layers III and II, which were near the ear position, consistent with previous reports (e.g., Li et al., 2019). Our results indicated that P_n decreased consistently from the top to the bottom layers (Fig. 4), which may have been related to leaf senescence and/or low light conditions in the lower canopy (Escobar-Gutiérrez and Combe, 2012; Hikosaka et al., 2016). High planting density places a great number of leaves in a shaded environment, which can restrict leaf development and photosynthesis, ultimately limiting biomass and yield (Raza et al., 2019). Increased planting density primarily reduced P_n and pigment contents among leaves in layers I and II (Fig. 4, Fig. 5). This implied that the functional traits of leaves in the lower layers were more severely compromised than those in the upper layers. Thus, increasing the planting density reduced biomass accumulation by a greater margin in layers I and II than in layers III or IV. Statistical analysis revealed positive associations of ear weight and per-plant biomass accumulation with biomass accumulation, P_n, and total chlorophyll contents in layers I and II specifically (Fig. 8), similar to earlier findings (Zhao et al., 2015). Collectively, these results suggested that photosynthetic production in layers I and II were the primary contributors to increases in grain yield due to high planting density.

Both planting density and maize variety had significant impacts on yield, kernel number, and 1000-kernel weight (Table 2). Under high-density planting, kernel number generally contributes more to yield variations than any related parameters do, including 1000-kernel weight (Andrade et al., 1999). A previous study reported that kernel number is mainly determined by floret number, which varies by genotype (Cárcova et al., 2000). However, specific conditions (e.g., planting density) can also affect kernel number by affecting floret degradation and kernel set (Rossini et al., 2011). In the present study, increasing planting density delayed the time to silking by up to 2–8 d; this corresponded to increased ASI and decreased ear length (Fig. 6, Supplementary Fig. S8, Supplementary Table S2).

Many studies have shown that kernel number is also affected by photosynthetic capacity and photoassimilate accumulation (Otegui et al., 1998; Cui et al., 2015). Carbohydrates, including sugars and starches, are dependent on photoassimilates from source organs and are the main sources for reproductive development (Macneill et al., 2017; Gustin et al., 2018). Sugars also act as signaling molecules, regulating the expression of various genes involved in metabolic pathways and cellular functions (Valluru, 2015; Hans-Wilhelm et al., 2018; Ruben et al., 2018). Low photosynthetic capacity in the leaves and the resulting insufficient assimilate supply can cause poor ear development, exacerbating yield losses (Hu et al., 2022; Pawar and Rana, 2019). In the present study, increasing the planting density increased starch content in the ears, but reduced levels of soluble sugars, especially glucose and fructose (Fig. 7). This suggested that increased planting density may have reduced ear metabolism, inhibiting development and thus yield. Moreover, due to the role of glucose as the main component of cell wall polysaccharides, low levels of this sugar may reduce the cellular growth rate (Shao et al., 2018). The observed low glucose levels may therefore have been responsible for reductions in ear length and diameter (Fig. 6, Supplementary Fig. S8), which were significantly positively correlated with kernel number (Supplementary Fig. S8, G to I). In addition, we found that increasing the planting density significantly impacted the ear, but not the tassel (Fig. 6, Supplementary Fig. S9, Supplementary Table S2). We hypothesized that this discrepancy was due to more intense intra-species competition during stages in which the ear was developing (V9–VT) than during stages in which the tassel was developing (V6–V12). Notably, the tassel is also located at the top of the canopy, which shows fewer density-dependent effects.

In conclusion, the results of this study indicated that high planting density was associated with decreased photosynthetic capacity of leaves within the lower canopy, which led to decreased biomass production. Furthermore, increased planting density suppressed ear development. These influences on both the leaves and the ears resulted in significant per-plant yield loss. Thus, strategies for maximizing grain yield under high-density planting conditions should focus on two key areas: optimizing the canopy structure to maintain high photosynthetic efficiency in the lower-canopy leaves and stimulation of ear development (Fig. 9). Moreover, we characterized the maize ideotype for high planting density, that the leaf length and width should be reduced in the upper canopy facilitating light penetration into the lower canopy, to further benefit the photosynthesis in the lower canopy with increased leaf length and slightly decreased leaf width. Our study not only provides mechanistic insights into biochemical processes affecting grain yield under high-density conditions, but establishes critical target traits for future maize breeding efforts, ultimately contributing to the development of high-yield maize and thus food security.

Materials and Methods

Plant materials and experimental design

Field experiments were conducted at the Wangtai Experimental Station of Ningxia Academy of Agricultural and Forestry Sciences, Ningxia, China (106º 14′ E, 38º 14′ N). Experiments were carried out during the growing seasons of 2019 and 2020 (Supplementary Fig. S1). The field site was located in the arid and semi-arid region of northwest China, in the irrigated zone for spring maize (*Zea mays* L.). Precipitation was monitored with a Watchdog portable-meteorological station (Watchdog 2900ET, Spectrum Technologies Inc., Aurora, IL, USA). The soil type was light sierozem, with 73.4 mg/kg alkali-hydrolyzable nitrogen, 66.0 mg/kg available phosphorus (Olsen-P), 313.8 mg/kg available potassium (NH_4Ac-K), 1.46 g/kg total nitrogen, and 17.3 g/kg organic matter in the 0–20 cm soil layer. After harvesting in 2018, 150 kg/ha diammonium phosphate (DAP) (containing 18% N and 20% P) was applied in combination with deep plowing and winter irrigation. Base fertilizers were applied prior to sowing, containing 225 kg N/ha (urea), 300 kg P_2O_5/ha (super phosphate), and 150 kg K_2O/ha (potassium sulfate). Additional fertilizer (225 kg N/ha [urea]) was applied at the silking stage. Diffuse irrigation was conducted four times during the growing period.

The maize cultivars ‘Liangyu 66’ (LY66), ‘Jingke 968’ (JK968) and ‘MC670’ were selected for the field experiments due to their high yield under different planting densities. Maize was sown at three densities (D1–D3) on 25th April 2019 and at four densities (D1–D4) on 15th April 2020. Rows were spaced 60 cm apart; spacing within each row was adjusted to reach the appropriate density. Three experimental plots per treatment with the split–split plot design was conducted each year, with planting density and cultivars as the main plot and subplot, respectively. Weeds, diseases, and pests were well-controlled by applicating pesticide within the plots.

For canopy profiling, aerial plant tissues were vertically divided into four layers based on the ear position; the upper and lower parts of the ear were divided into two layers (Supplementary Fig. S2). All organs were measured in their natural state within the canopy. The four canopy layers were designated I–IV from the bottom of the plant to the top. The leaf located in the middle of each layer was selected as the representative leaf for gas exchange and pigment measurements as described below.

Grain yield and lodging rate measurements

The 1000-kernel weight and kernel number were measured at physiological maturity.

Plants in the middle of each plot were selected for these measurements and 20 ears per plot were gathered. Measurements were taken after the ears were air dried. To measure grain yield, a 12-m^2 region in the middle of a plot was selected; all plants within that region were harvested to form a single biological replicate. Samples were dried and the grain moisture content was standardized (14%) before yield was calculated. Three biological replicates were analyzed per treatment group in 2019 and 2020. The plant lodging rate was calculated as the percentage of lodged plants out of the total plant number per plot. Four replicates were performed for each treatment in 2020.

Biomass accumulation and transfer measurements

Plant aerial tissues were vertically divided into four layers. Leaves, stems (including the internodes, sheaths, and tassels), and ears (including the husks, cobs, and kernels) of each layer were collected from three or four representative plants per group at the silking and maturity stages in 2019 and 2020. Tissues were separated and oven-dried to a constant weight, which was recorded as the dry weight (DW). The sum of all parts for each plant was considered the accumulated biomass. There were three to four independent replicates per group. Biomass transfer was calculated as described by Wang et al. (2021): subtraction of the biomass accumulation in nutritional organs at maturity from the biomass accumulation in nutritional organs at the silking stage.

Leaf area and light measurements

At the silking stage, three representative plants per group were selected for leaf area measurements in 2019 and 2020. Leaves at every position were measured to determine the maximum leaf width (W) and the leaf length (L). The leaf area (S) was then calculated as follows:

$$S = 0.75 \times L \times W$$

SDLA was calculated as the leaf area index divided by the plant height at each layer. Light measurements were taken in each layer at 655–665 nm (red) and 725–735 nm (far red) with a SpectraPen LM500 hand-held spectrometer (Photon Systems Instruments, Drásov, Czechia) on a sunny, cloudless day. Three replicates were measured for each treatment in 2020. Using these measurements, R/FR was calculated as irradiance in the red band divided by irradiance in the far-red band. Canopy transmission was calculated as follows:

$$\text{Transmission (\%)} = \text{PAR}_n / \text{PAR}_{top} \times 100$$

where PAR_n is PAR in each layer and PAR_{top} is PAR above canopy. The photosynthetically active radiation (PAR) was measured for each layer at the silking stage on a clear day from 11:00–13:00 with a SunScan line quantum sensor (Delta-T Devices, Cambridge, UK). Interception of photosynthetically active radiation (IPAR) corresponded to PAR_n minus PAR_{n-1} and was then used to calculate FIPAR as follows:

$$\text{FIPAR} = \text{IPAR} / \text{PAR}_n$$

Gas exchange measurements

P_n was measured at the silking stage using the LI-6400XT portable photosynthesis system equipped with an LED leaf chamber (Li-Cor Inc., Lincoln, NE, USA). Measurements were taken for the representative leaf in each canopy layer. The photosynthetic photon flux density (PPFD) was assumed to be 2000 μmol photons m^{-2} s^{-1} on sunny days. Measurements were taken in three replicate plants in 2019 and four replicate plants in 2020 per group.

Pigment measurements

In each canopy layer, the selected representative leaf from three plants per group was collected at the silking stage in 2019 and 2020, and frozen at -80 °C. After freezing, each leaf was homogenized via milling, then combined with 1 mL of acetone (100%). Samples were incubated in acetone at 4 °C until all pigments were removed from the leaf tissue. Samples were centrifuged for 10 min at 4 °C and 10,000 × g. After collection of the supernatant, samples were measured using a Ultrospec 8000PC dual-beam spectrophotometer (Biochrom Ltd., Cambridge, UK). These measurements were used to calculate the total carotenoid and chlorophyll contents in each sampled leaf as previously described (Lichtenthaler, 1987). Total chlorophyll content was calculated as the sum of chlorophyll *a* and chlorophyll *b* content.

Tassel and ear development and flowering rate

Four representative plants from D1 and D4 plot were harvested at 2–3 d intervals beginning at the 10th-leaf (V10) stage to assess the tassel and ear developmental processes in 2020. The growth cone was stripped with a dissecting needle, then fixed with formaldehyde/alcohol/acetic acid (FAA) solution. The tassels and ears were photographed with a DSC-WX300 digital camera (Sony Corporation, Tokyo, Japan) and a SteREO Discovery V8 stereoscopic microscope (ZEISS, Oberkochen, Germany). The tassel and ear lengths were also measured.

Before anthesis, plants within a 6-m^2 area of each plot were labeled. The number of silking ears was then recorded after 16:00 every day. When the percentage of silking ears reached ≥ 60% for the first time, the plot was recorded as having reached the silking stage.

Sucrose, glucose, fructose, and starch content measurements

Ear cones from D1 and D4 groups were harvested at 72 d after sowing and 77 d after sowing in 2020, then frozen at -80 °C. The materials were ground to a fine, homogeneous powder with liquid nitrogen. Sugars were extracted from 30 mg of milled ear cone per sample and measured with a sucrose/D-fructose/D-glucose detection kit (K-SUFRG) and a total starch detection kit (K-TSTA) (both from Megazyme, Bray, Ireland).

Statistical analyses

Data were processed in Microsoft Excel 2016. Differences between groups were analyzed with two-way analysis of variance (ANOVA). Least significant difference (LSD) multiple comparison and correlation analyses were performed in SPSS 21.0 (SPSS Institute Inc., Chicago, IL, USA). Differences were considered statistically significant at $p < 0.05$. Figures were generated in GraphPad Prism 8 (GraphPad, San Diego, CA, USA).

Funding

This work was supported by the National Key Research and Development Program of China (2016YFD0300102). W.Z. was supported by the Innovation Program of the Chinese Academy of Agricultural Sciences and the Elite Youth Program of the Chinese Academy of Agricultural Sciences. X.L. was supported by the Open Project Funding of the State Key Laboratory of Crop Stress Adaptation and Improvement.

Acknowledgments

We would like to thank Wenjie Zhang and Qiming Cai (Ningxia Academy of Agriculture and Forestry Sciences) and our colleagues from Institute of Crop Sciences for kindly assistance during the experiment.

Author contributions

W.Z. and Y.Y. conceived and designed the experiments; Y.Y., R.Z. and Y.W. performed the experiments; P.H., M.Z., S.L. and T.D. helped with the field experiments; Y.Y., F.D., X.L. and W.Z. wrote the manuscript. All authors contributed to data evaluation and interpretation of this article.

Tables

Table 1. Grain yield components and associated parameters in three maize varieties at several planting densities in 2019 and 2020

Year	Cultivar	Planting density	Grain Yield (t/ha)	Grain weight per plant (g)	Ear # (× 10^3/ha)	Kernel #	1000-kernel weight (g)	Pop. biomass (t/ha)	HI	Barren stalk rate (%)	Lodging rate (%)
2019	LY66	D1	18.6 ± 0.17^{c}	267.8 ± 11.1^{a}	73.15 ± 1.60^{c}	641.89 ± 9.19^{b}	417.12 ± 14.02^{a}	34.38 ± 1.01^{c}	0.54 ± 0.01^{a}	0 ± 0^{b}	-
		D2	19.8 ± 0.7^{bc}	206.5 ± 7.9^{bc}	100.00 ± 2.78^{b}	563.85 ± 23.95^{de}	381.55 ± 8.00^{b}	40.30 ± 1.34^{b}	0.49 ± 0.00^{b}	3.56 ± 1.48^{a}	-
		D3	19.5 ± 1.0^{bc}	197.8 ± 4.7^{c}	112.04 ± 1.60^{a}	535.96 ± 5.93^{e}	369.01 ± 7.22^{bc}	39.07 ± 0.98^{b}	0.50 ± 0.02^{b}	4.72 ± 0.06^{a}	-
	MC670	D1	19.8 ± 0.9^{bc}	270.9 ± 13.4^{a}	76.85 ± 3.21^{c}	675.10 ± 19.17^{a}	401.13 ± 9.98^{a}	35.43 ± 0.26^{c}	0.56 ± 0.02^{a}	-1.19 ± 2.06^{b}	-
		D2	21.4 ± 0.6^{a}	227.0 ± 16.6^{b}	103.70 ± 1.60^{b}	605.20 ± 15.04^{c}	371.12 ± 5.37^{bc}	42.79 ± 0.13^{a}	0.50 ± 0.01^{b}	3.44 ± 1.46^{a}	-
		D3	20.8 ± 1.2^{ab}	206.9 ± 9.6^{bc}	114.81 ± 6.42^{a}	576.43 ± 21.94^{d}	358.94 ± 3.06^{c}	40.96 ± 1.34^{ab}	0.51 ± 0.02^{b}	3.88 ± 2.68^{a}	-
2020	LY66	D1	17.5 ± 0.3^{cde}	228.4 ± 9.0^{a}	75.93 ± 1.60^{g}	569.20 ± 14.06^{bc}	401.19 ± 8.92^{a}	32.41 ± 0.28^{i}	0.54 ± 0.01^{a}	0 ± 0^{a}	-
		D2	19.9 ± 1.1^{ab}	209.3 ± 9.1^{cd}	105.56 ± 2.78^{e}	552.53 ± 18.23^{c}	378.63 ± 4.04^{bc}	38.50 ± 1.04^{bcd}	0.52 ± 0.02^{abc}	0 ± 0^{a}	-
		D3	18.5 ± 1.6^{bc}	187.3 ± 1.8^{ef}	114.81 ± 1.60^{cd}	524.80 ± 3.27^{d}	361.13 ± 4.58^{def}	37.08 ± 1.25^{def}	0.50 ± 0.03^{bcd}	3.10 ± 2.69^{bc}	-
		D4	17.8 ± 0.6^{cde}	173.6 ± 4.2^{g}	124.12 ± 1.64^{b}	494.13 ± 3.84^{e}	351.37 ± 6.47^{fg}	36.23 ± 0.69^{ef}	0.49 ± 0.01^{cd}	3.56 ± 1.24^{bc}	-
	MC670	D1	17.9 ± 0.3^{cde}	223.1 ± 10.3^{ab}	73.15 ± 1.60^{gh}	580.37 ± 13.35^{b}	384.48 ± 14.07^{b}	33.00 ± 1.18^{hi}	0.54 ± 0.02^{a}	0 ± 0^{a}	-
		D2	21.0 ± 0.1^{a}	210.4 ± 5.3^{cd}	102.78 ± 0.00^{ef}	571.77 ± 7.31^{bc}	368.05 ± 7.21^{cde}	39.64 ± 0.52^{ab}	0.53 ± 0.01^{ab}	0.88 ± 1.52^{ab}	-
		D3	19.9 ± 1.0^{ab}	197.2 ± 7.3^{de}	117.59 ± 1.60^{c}	559.40 ± 15.32^{bc}	354.11 ± 3.01^{efg}	40.16 ± 0.22^{a}	0.49 ± 0.03^{bcd}	0.78 ± 1.34^{ab}	-
		D4	18.6 ± 0.9^{bc}	175.4 ± 5.1^{g}	128.70 ± 1.60^{a}	512.11 ± 5.60^{de}	342.43 ± 7.94^{g}	39.02 ± 1.04^{abc}	0.48 ± 0.01^{d}	2.10 ± 2.08^{abc}	-
	JK968	D1	16.8 ± 1.0^{cde}	232.8 ± 9.4^{a}	72.22 ± 2.78^{h}	609.70 ± 8.57^{a}	381.79 ± 10.18^{bc}	33.85 ± 1.26^{hi}	0.49 ± 0.02^{bcd}	0 ± 0^{a}	72.22 ± 5.09^{b}
		D2	18.2 ± 0.9^{bcd}	213.8 ± 13.9^{bc}	101.85 ± 1.60^{f}	574.77 ± 27.23^{bc}	371.85 ± 8.25^{bcd}	37.56 ± 0.62^{cde}	0.48 ± 0.02^{cd}	0.88 ± 1.52^{ab}	89.17 ± 8.04^{a}
		D3	16.4 ± 1.1^{de}	179.0 ± 6.1^{fg}	113.89 ± 2.78^{d}	501.33 ± 20.16^{e}	357.14 ± 10.11^{efg}	35.66 ± 0.48^{fg}	0.46 ± 0.03^{d}	3.91 ± 1.38^{c}	82.05 ± 2.22^{ab}
		D4	16.1 ± 1.6^{e}	161.1 ± 7.8^{h}	125.93 ± 1.60^{ab}	466.67 ± 22.43^{f}	345.18 ± 0.74^{g}	34.29 ± 0.70^{gh}	0.47 ± 0.04^{d}	4.21 ± 2.06^{c}	87.50 ± 6.61^{a}

Pop. biomass, population-scale biomass accumulation at maturity; HI, harvest index. Data are presented as the mean ± standard deviation (SD) from three biological replicates parameter for each variety and year. Lowercase letters indicate statistical significance groups at $p < 0.05$ (two-way analysis of variance).

Table 2. Effects of maize variety and planting density on yield and related parameters in 2019 and 2020

Variable	**Effect of variety (V) in 2019**	**Effect of planting density (D) in 2019**	**Effect of V × D in 2019**	**Effect of V in 2020**	**Effect of D in 2020**	**Effect of V × D in 2020**
Grain yield	14.3**	5.1*	0.09	17.9**	9.8**	0.68
Grain weight per plant	1.5	44.8**	0.12	1.6	117.7**	3.1*
Ear number	5.171*	232.436**	0.043	3.989*	1277.445**	3.234*
Kernel number	26.475**	66.983**	0.12	9.322**	99.089**	9.006**
1000-kernel weight	7.686*	37.703**	0.191	6.304**	48.637**	0.585
Pop. biomass	14.341**	70.906**	0.751	29.13**	68.53**	6.953**
HI	2.34	19.3**	0.13	11.23**	10.44**	0.71
Barren stalk rate	0.775	13.852**	0.151	2.245	9.65**	1.016

Pop. biomass, population biomass at maturity; HI, harvest index. Effect sizes shown are the F values from two-way analysis of variance. *$p < 0.05$; **$p < 0.01$ (two-way analysis of variance).

Figures and legends

Figure 1. Biomass accumulation in each maize canopy layer among plants grown at several planting densities.

(**A–E**) Biomass accumulation at the silking stage for (**A**) LY66 in 2019, (**B**) MC670 in 2019, (**C**) LY66 in 2020, (**D**) MC670 in 2020, and (**E**) JK968 in 2020. (**F–J**) Biomass accumulation at the maturity stage for (**F**) LY66 in 2019, (**G**) MC670 in 2019, (**H**) LY66 in 2020, (**I**) MC670 in 2020, and (**J**) JK968 in 2020. D1–D4 represent 75,000, 105,000, 120,000, and 135,000 plants/ha, respectively. Lowercase letters indicate statistical significance groups at $p < 0.05$ (two-way analysis of variance with post-hoc least significant difference test). Data are presented as the mean ± standard error from three or four biological replicates per group.

Figure 2. Biomass transfer in each maize canopy layer among plants grown at several planting densities.

(**A–E**) Biomass transfer before the silking stage in (**A**) LY66 in 2019, (**B**) MC670 in 2019, (**C**) LY66 in 2020, (**D**) MC670 in 2020, and (**E**) JK968 in 2020. A negative value indicates that the dry weight was higher at maturity than at the silking stage. The transfer amount was calculated from biomass accumulation per plant. D1–D4 represent 75,000, 105,000, 120,000, and 135,000 plants/ha, respectively. Lowercase letters indicate statistical significance groups at $p < 0.05$ (two-way analysis of variance with post-hoc least significant difference test). Data are presented as the mean ± standard error from three or four biological replicates per group.

Figure 3. Green leaf area at each leaf position among plants grown at several planting densities.

(**A–E**) Green leaf area at each leaf position at the silking stage in (**A**) LY66 in 2019, (**B**) MC670 in 2019, (**C**) LY66 in 2020, (**D**) MC670 in 2020, and (**E**) JK968 in 2020. The first visible complete leaf was the seventh leaf from the bottom at the silking stage. Numbers 7–21 indicate the seventh to 21st leaves, respectively, from the bottom of the plant. Black dotted lines represent the ear position. D1–D4 correspond to

75,000, 105,000, 120,000, and 135,000 plants/ha, respectively. Data are presented as the mean ± standard error from three biological replicates per group.

Figure 4. Net photosynthesis (P_n) in the leaves of each canopy layer among plants grown at several planting densities.

(**A–E**) P_n at the silking stage in (**A**) LY66 in 2019, (**B**) MC670 in 2019, (**C**) LY66 in 2020, (**D**) MC670 in 2020, and (**E**) JK968 in 2020. D1–D4 represent 75,000, 105,000, 120,000, and 135,000 plants/ha, respectively. P_n, net photosynthetic rate. Lowercase letters indicate statistical significance groups at $p < 0.05$ (two-way analysis of variance with post-hoc least significant difference test). Data are presented as the mean ± standard error from three or four biological replicates per group.

Figure 5. Total chlorophyll contents in leaves from each canopy layer among plants grown at several planting densities.

(**A–E**) Total chlorophyll contents in leaves at silking stage in (**A**) LY66 in 2019, (**B**) MC670 in 2019, (**C**) LY66 in 2020, (**D**) MC670 in 2020, and (**E**) JK968 in 2020. D1–D4 represent 75,000, 105,000, 120,000, and 135,000 plants/ha, respectively. Lowercase letters indicate statistical significance groups at $p < 0.05$ (two-way analysis of variance with post-hoc least significant difference test). Data are presented as the mean ± standard error from three biological replicates per group.

Figure 6. Young ear development among plants grown at several planting densities.

(**A, C, E**) Representative (**A**) LY66, (**C**) MC670, and (**E**) JK968 ears at several time points after sowing in 2020. Images were digitally extracted for comparison. (**B, D, F**) Quantification of ear length over time for (**B**) LY66, (**D**) MC670, and (**F**) JK968 plants. Scale bar = 1 cm. DAS, days after sowing. D1, 75,000 plants/ha; D4, 135,000 plants/ha. *$p < 0.05$, **$p < 0.01$ (Student's *t*-test). ns, not significant. Data are presented as the mean ± standard error from four biological replicates per group.

Figure 7. Levels of starch, sucrose, glucose, and fructose in young maize ears from plants grown at several planting densities.

(**A–D**) Levels of (**A**) starch, (**B**) sucrose, (**C**) glucose, and (**D**) fructose. Samples were analyzed at 72 and 77 d after sowing in 2020. DAS, days after sowing. D1, 75,000 plants/ha; D4, 135,000 plants/ha. Lowercase letters indicate statistical significance groups at $p < 0.05$ (two-way analysis of variance with post-hoc least significant difference test). Data are presented as the mean ± standard error from three or four biological replicates per group, each of which consisted of pooled samples from at least three plants.

Figure 8. Correlation of yield components with physiological parameters at each canopy layer among plants grown at several planting densities.

(**A**–**B**) Correlation of yield with (**A**) kernel number and (**B**) biomass accumulation at maturity. (**C**–**G**) Correlation of grain weight per plant with (**C**) biomass accumulation per plant at silking, (**D**) biomass accumulation per plant at maturity, (**E**) biomass transfer per plant, (**F**) FIPAR in layer III and (**G**) P_n. (**H**–**I**) Correlation of biomass accumulation per plant at maturity in (**H**) layer I and (**I**) layer II with P_n. (**J**) Correlation of grain weight per plant with chlorophyll content in layer II. $^*p < 0.05$, $^{**}p < 0.01$ (Pearson correlation analysis). FIPAR, fractional interception of photosynthetically active radiation; P_n, net photosynthetic rate. (**A–E**) and (**G–I**) A total of 54 replicates, each point represents one replicate of one planting density and one variety and one year; (F) and (**J**) A total of 18 replicates, each point represents one planting density of one variety and one year. (**A–B**) Data are based on the entire canopy; (**C–J**) Data are based on different canopy layers.

Figure 9. Schematic diagram showing the physiological mechanisms of yield losses or gains among plants grown at several planting densities.

Representations of (**A**) reduced and (**B**) increased grain yield under high-density planting conditions. Increased planting density reduces the photosynthetic rate and leaf area in the lower canopy layer, thereby reducing assimilate accumulation. Moreover, increased planting density affects the glucose and fructose contents of young ears, impairing ear development. This ultimately reduces kernel number per ear and per-plant kernel weight, resulting in per-plant yield losses. Optimizing leaf morphology in the canopy layers in response to increased planting density could improve the photosynthetic rate and stimulate ear development, increasing yield. The dashed boxes represent the parts of below and above ear in the plant. Processes named in turmeric, blue, and black correspond to ear development, carbon metabolism, and yield, respectively. The black arrows represent the indication. Blue arrows (regular solid arrows and outline arrow) and purple outline arrow represent decreases and increases, respectively, in the indicated processes.

Declarations

Conflict of interest The authors declare they have no conflicts of interest in this paper.

References

Allison JCS, Watson DJ (1966) The production and distribution of dry matter in maize after flowering. Ann Bot **30:** 365-381.

Andrade FH, Vega C, Uhart S, Cirilo A, Cantarero M, Valentinuz O (1999) Kernel number determination in maize. Crop Sci **39(2)**: 453-459.

Andrea S, Di BD, Pierangelo B, Olga G, Giorgio M (2016) Investigating the European beech (*Fagus sylvatica* L.) leaf characteristics along the vertical canopy profile: leaf structure, photosynthetic capacity, light energy dissipation and photoprotection mechanisms. Tree Physiol **36(9):** 1060-1076.

Assefa Y, Carter P, Hinds M, Bhalla G, Schon R, Jeschke M, Paszkiewicz S, Smith S, Ciampitti IA (2018) Analysis of long term study indicates both agronomic optimal plant density and increase maize yield per plant contributed to yield gain. Sci Rep **8:** 4937.

Cárcova J, Uribelarrea M, Borrás L, Otegui ME, Westgate ME (2000) Synchronous pollination within and between ears improves kernel set in maize. Crop Sci **40(4):** 1056-1061.

Chen W, Zhang J, Deng X (2019) The spike weight contribution of the photosynthetic area above the upper internode in a winter wheat under different N and mulching regimes. Crop J **7:** 89-100.

Chen Y, Wu D, Mu X, Xiao C, Chen F, Yuan L, Mi G (2015) Vertical distribution of photosynthetic nitrogen use efficiency and its response to nitrogen in field-grown maize. Crop Sci **56:** 397-407.

Ciampitti IA, Vyn TJ (2013) Grain nitrogen source changes over time in maize: a review. Crop Sci **53:** 366-377.

Collison RF, Raven EC, Pignon CP, Long SP (2020) Light, not age, underlies the maladaptation of maize and miscanthus photosynthesis to self-shading. Front Plant Sci **11:** 783.

Cui H, Camberato JJ, Jin L, Zhang J (2015) Effects of shading on spike differentiation and grain yield formation of summer maize in the field. Int J Biometeorol **59:** 1189-1200.

Deng J, Ran J, Wang Z, Fan Z, Wang G, Ji M, Liu J, Wang Y, Liu J, Brown JH (2012) Models and tests of optimal density and maximal yield for crop plants. Proc Natl Acad Sci U S A **109:** 15823-15828.

Duan F, Wei Z, Soualiou S, Zhou W (2023) Nitrogen partitioning in maize organs and underlined mechanisms from different plant density levels and N application rate in China. Field Crops Res **294:** 108874.

Escobar-Gutiérrez AJ, Combe L (2012) Senescence in field-grown maize: from flowering to harvest. Field Crops Res **134:** 47-58.

FAO (2021) Statistics for trade of crops and livestock products-dataset. https://www.fao.org/faostat/en/#data/QCL.

Gaju O, DeSilva J, Carvalho P, Hawkesford MJ, Griffiths S, Greenland A, Foulkes MJ (2016) Leaf photosynthesis and associations with grain yield, biomass and nitrogen-use efficiency in landraces, synthetic-derived lines and cultivars in wheat. Field Crops Res **193:** 1-15.

Guo Y, Yin W, Fan H, Fan Z, Hu F, Yu A, Zhao C, Chai Q, Aziiba EA, Zhang X (2021) Photosynthetic physiological characteristics of water and nitrogen coupling for enhanced high-density tolerance and increased yield of maize in arid irrigation regions. Front Plant Sci **12:** 726568.

Gustin JL, Boehlein SK, Shaw JR, Junior W, Settles AM, Webster A (2018) Ovary abortion is prevalent in diverse maize inbred lines and is under genetic control. Sci Rep **8:** 13032.

Hans-Wilhelm N, Claudio S, Anne O (2018) Metabolic gene clusters in eukaryotes. Annu Rev Genet **52(1):** 159-183.

Hikosaka K, Anten NP, Borjigidai A, Kamiyama C, Sakai H, Hasegawa T, Oikawa S, Iio A, Watanabe M, Koike T, Nishina K, Ito A (2016) A meta-analysis of leaf nitrogen distribution within plant canopies. Ann Bot **118:** 239-247.

Hu J, Ren B, Dong S, Liu P, Zhao B, Zhang J (2022) Poor development of spike differentiation triggered by lower photosynthesis and carbon partitioning reduces summer maize yield after waterlogging. Crop J **10(2):** 478-489.

Hu W, Lu Z, Meng F, Li X, Cong R, Ren T, Sharkey TD, Lu J (2020) The reduction in leaf area precedes that in photosynthesis under potassium deficiency: the importance of leaf anatomy. New Phytol **227:** 1749-1763.

Li Y, Song H, Zhou L, Xu Z, Zhou G (2019) Vertical distributions of chlorophyll and nitrogen and their associations with photosynthesis under drought and rewatering regimes in a maize field. Agr Forest Meteorol **272-273:** 40-54.

Lichtenthaler H (1987) Chlorolphylls and carotenoids: pigments of photosynthetic biomembranes. Method Enzymol **148:** 350-382.

Liu G, Yang Y, Guo X, Liu W, Xie R, Ming B, Xue J, Wang K, Li S, Hou P (2023) A global analysis of dry matter accumulation and allocation for maize yield breakthrough from 1.0 to 25.0 Mg ha^{-1}. Resour Conserv Recy **188:** 106656.

Luo N, Meng Q, Feng P, Qu Z, Yu Y, Liu D, Müller C, Wang P (2023) China can be self-sufficient in maize production by 2030 with optimal crop management. Nat Commun **14:** 2637.

Ma L, Li Y, Wu P, Zhao X, Gao X, Chen X (2020) Recovery growth and water use of intercropped maize following wheat harvest in wheat/maize relay strip intercropping. Field Crops Res **256:** 107924.

Macneill GJ, Sahar M, Minow MAA, Patterson JA, Tetlow IJ, Emes MJ (2017) Starch as a source, starch as a sink: the bifunctional role of starch in carbon allocation. J Exp Bot **68(16):** 4433-4453.

Mastrodomenico AT, Haegele JW, Seebauer JR, Below F (2018) Yield stability differs in commercial maize hybrids in response to changes in plant density, nitrogen fertility, and environment. Crop Sci **58(1):** 230-241.

Odorico PD, Emmel C, Revill A, Liebisch F, Eugster W, Buchmann N (2019) Vertical patterns of photosynthesis and related leaf traits in two contrasting agricultural crops. Funct Plant Biol **46(3):** 213-227.

Otegui ME, Bonhomme R (1998) Grain yield components in maize: I. Ear growth and kernel set. Field Crops Res **56(3):** 247-256.

Pagano E, Cela S, Maddonni GA, Otegui ME (2007) Intraspecific competition in maize: Ear development, flowering dynamics and kernel set of early-established plant hierarchies. Field Crops Res **102:** 198-209.

Parvathaneni RK, Bertolini E, Shamimuzzaman M, Vera DL, Lung PY, Rice BR, Zhang J, Brown PJ, Lipka AE, Bass HW, Eveland AL (2020) The regulatory landscape of early maize inflorescence development. Genome Biol **21(1):** 165.

Pawar R, Rana VS (2019) Manipulation of source-sink relationship in pertinence to better fruit quality and yield in fruit crops: A review. Agric Rev **40(3):** 200-207.

Perez R, Fournier C, Cabrera-Bosquet L, Artzet S, Tardieu F (2019) Changes in the vertical distribution of leaf area enhanced light interception efficiency in maize over generations of selection. Plant Cell Environ **42(7):** 2105-2119.

Prajal P, Günther F, Harrij VV, Reusser DE, Kropp JP, Luis GAJ. (2015). Closing yield gaps: How sustainable can we be? PLoS One **10(5):** e0129487.

Raza MA, Bin Khalid MH, Zhang X, Feng LY, Khan I, Hassan MJ, Ahmed M, Ansar M, Chen YK, Fan YF, Yang F, Yang W (2019) Effect of planting patterns on yield, nutrient accumulation and distribution in maize and soybean under relay intercropping systems. Sci Rep **9(1):** 4947.

Rossini MA, Maddonni GA, Otegui ME (2011) Inter-plant competition for resources in maize crops grown under contrasting nitrogen supply and density: Variability in plant and ear growth. Field Crops Res **121(3):** 373-380.

Ruben V, Omar VD, Susan M, Fadia C, Kefauver SC, Jordi B, Dolores SM, Nieves A, Luis AJ (2018) Durum wheat ears perform better than the flag leaves under water stress: Gene expression and physiological evidence. Environ Exp Bot **153:** 271-285.

Sarlikioti V, de Visser PH, Buck-Sorlin GH, Marcelis LF (2011) How plant architecture affects light absorption and photosynthesis in tomato: towards an ideotype for plant architecture using a functional-structural plant model. Ann Bot **108(6):**1065-1073.

Shao D, Villet O, Zhang Z, Choi SW, Yan J, Ritterhoff J, Gu HW, Djukovic D, Christodoulou D, Kolwicz Jr S, Raftery D, Tian R (2018) Glucose promotes cell growth by suppressing branched-chain amino acid degradation. Nat Commun **9:** 2935.

Sher A, Khan A, Li JC, Ahmad MI, Jamoro SA (2017) Response of maize grown under high plant density; performance, issues and management - A critical review. Adv Crop Sci Tech **5:** 275.

Simkin AJ, Lopez-Calcagno PE, Raines CA (2019) Feeding the world: improving photosynthetic efficiency for sustainable crop production. J Exp Bot **70:** 1119-1140.

Slattery RA, Walker BJ, Weber APM, Ort DR (2018) The impacts of fluctuating light on crop performance. Plant Physiol **176(2):** 990-1003.

Song H, Li Y, Zhou L, Xu Z, Zhou G (2018) Maize leaf functional responses to drought episode and rewatering. Agric For Meteorol **249:** 57-70.

Sultana F, Dev W, Xin M, Han Y, Feng L, Lei Y, Yang B, Wang G, Li X, Wang Z, Xing F, Xiong S, Li Y (2023) Competition for light interception in different plant canopy characteristics of diverse cotton cultivars. Genes (Basel) **14(2):**364.

Tian X, Engel BA, Qian H, Hua E, Sun S, Wang Y (2021) Will reaching the maximum achievable yield potential meet future global food demand? J Clean Prod **294:** 1-12.

Timlin DJ, Fleisher DH, Kemanian AR, Reddy VR (2014) Plant density and leaf area index effects on the distribution of light transmittance to the soil surface in maize. Agron J **106(5):** 1828-1837.

Uribelarrea M, Cárcova J, Borrás L, Otegui ME (2008) Enhanced kernel set promoted by synchronous pollination determines a tradeoff between kernel number and kernel weight in temperate maize hybrids. Field Crops Res **105:**172-181.

Valluru R (2015) Fructan and hormone connections. Front Plant Sci **6:** 180.

Wang F, Xie R, Ming B, Wang K, Hou P, Chen J, Liu G, Zhang G, Xue J, Li S

(2021) Dry matter accumulation after silking and kernel weight are the key factors for increasing maize yield and water use efficiency. Agric Water Manag **254:** 106938.

Wei H, Kong D, Yang J, Wang H (2020) Light regulation of stomata development and patterning: shifting the paradigm from Arabidopsis to grasses. Plant Commun **1(2):** 9.

Wilson JH, Allison JCS (1978) Effect of plant population on ear differentiation and growth in maize. Ann Appl Biol **90:** 127-132.

Xin Q, Zhang L, Qu Y, Geng H, Li X, Peng S (2023) Satellite mapping of maize cropland in one-season planting areas of China. Sci Data **10:** 437.

Xu Z, Zhou G, He Q (2021) Vertical distribution of gas exchanges and their integration throughout the entire canopy in a maize field. Photosyn Res **147(3):** 269-281.

Yan Y, Hou P, Duan FY, Niu L, Dai T, Wang K, Zhao M, Li S, Zhou W (2021) Improving photosynthesis to increase grain yield potential: an analysis of maize hybrids released in different years in China. Photosyn Res **150:** 295-311.

Zhang D, Sun Z, Feng L, Bai W, Zhang L (2020) Maize plant density affects yield, growth and source-sink relationship of crops in maize/peanut intercropping. Field Crops Res **257:** 107926.

Zhang J, Peng Z, Li T (2009) Effects of different N application rates on the dynamic accumulation and distribution of assimilate and N content in maize. Journal of Hebei Agricuture University **2:** 1-5 (in Chinese with English abstract).

Zhang M, Chen T, Hojatollah L (2018) How plant density affects maize spike differentiation, kernel set, and grain yield formation in northeast China? J Integr Agric **17:** 53-65.

Zhang P, Xia L, Sun Z, Zhang T (2023) Analysis of spatial and temporal changes and driving forces of arable land in the Weibei dry plateau region in China. Sci Rep **13:** 20618.

Zhang Y, Wang R, Wang S, Ning F, Li J (2019) Effect of planting density on deep soil water and maize yield on the Loess Plateau of China. Agric Water Manag **223:** 105655.

Zhao J, Yang X, Lin X, Sassenrath GF, Dai S, Lv S, Chen X, Chen F, Mi G (2015) Radiation interception and use efficiency contributes to higher yields of newer maize hybrids in northeast China. Agron J **107(4):** 1473-1480.

Zheng M, Chen J, Shi Y, Li Y, Yin Y, Yang D, Luo Y, Pang D, Xu X, Li W, Ni J, Wang Y, Wang Z, Li Y (2017) Manipulation of lignin metabolism by plant densities and its relationship with lodging resistance in wheat. Sci Rep **7:** 41805.

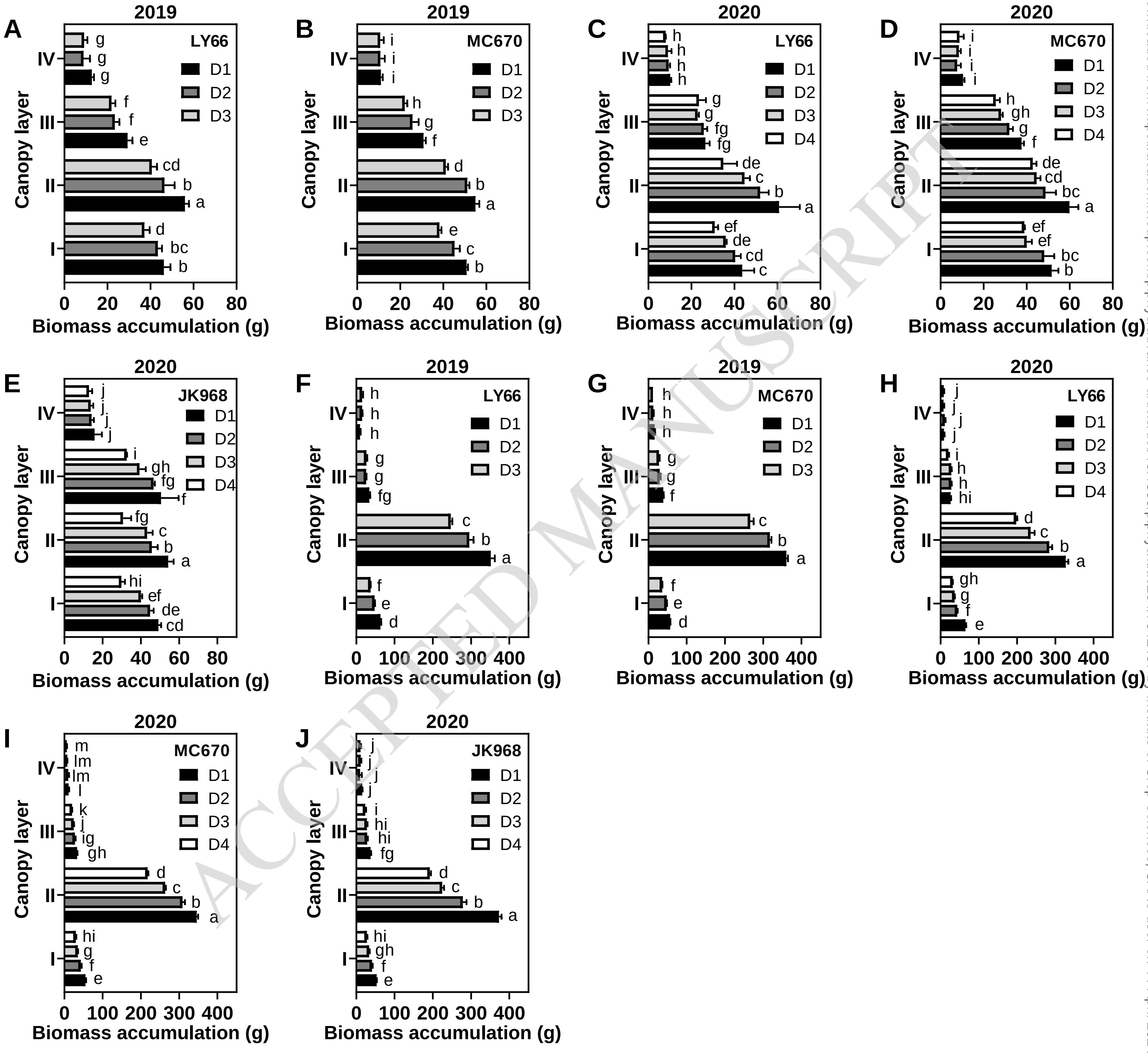

A
2019
LY66
D1
D2
D3
Canopy layer
IV
III
II
I
g g g
f f e
cd b a
d bc b
0 20 40 60 80
Biomass accumulation (g)
B
2019
MC670
D1
D2
D3
i i i
h g f
d b a
e c b
Canopy layer
Biomass accumulation (g)
C
2020
LY66
D1
D2
D3
D4
h h h h
g g fg fg
de c b a
ef de cd c
Canopy layer
Biomass accumulation (g)
D
2020
MC670
D1
D2
D3
D4
i i i i
h gh g f
de cd bc a
ef ef bc b
Canopy layer
Biomass accumulation (g)
E
2020
JK968
D1
D2
D3
D4
j j j j
i gh fg f
fg c b a
hi ef de cd
Canopy layer
Biomass accumulation (g)
F
2019
LY66
D1
D2
D3
h h h
g g fg
c b a
f e d
0 100 200 300 400
Canopy layer
Biomass accumulation (g)
G
2019
MC670
D1
D2
D3
h h h
g g f
c b a
f e d
Canopy layer
Biomass accumulation (g)
H
2020
LY66
D1
D2
D3
D4
j j j j
i h h hi
d c b a
gh g f e
Canopy layer
Biomass accumulation (g)
I
2020
MC670
D1
D2
D3
D4
m lm lm l
k j ig gh
d c b a
hi g f e
Canopy layer
Biomass accumulation (g)
J
2020
JK968
D1
D2
D3
D4
j j j j
i hi hi fg
d c b a
hi gh f e
Canopy layer
Biomass accumulation (g)

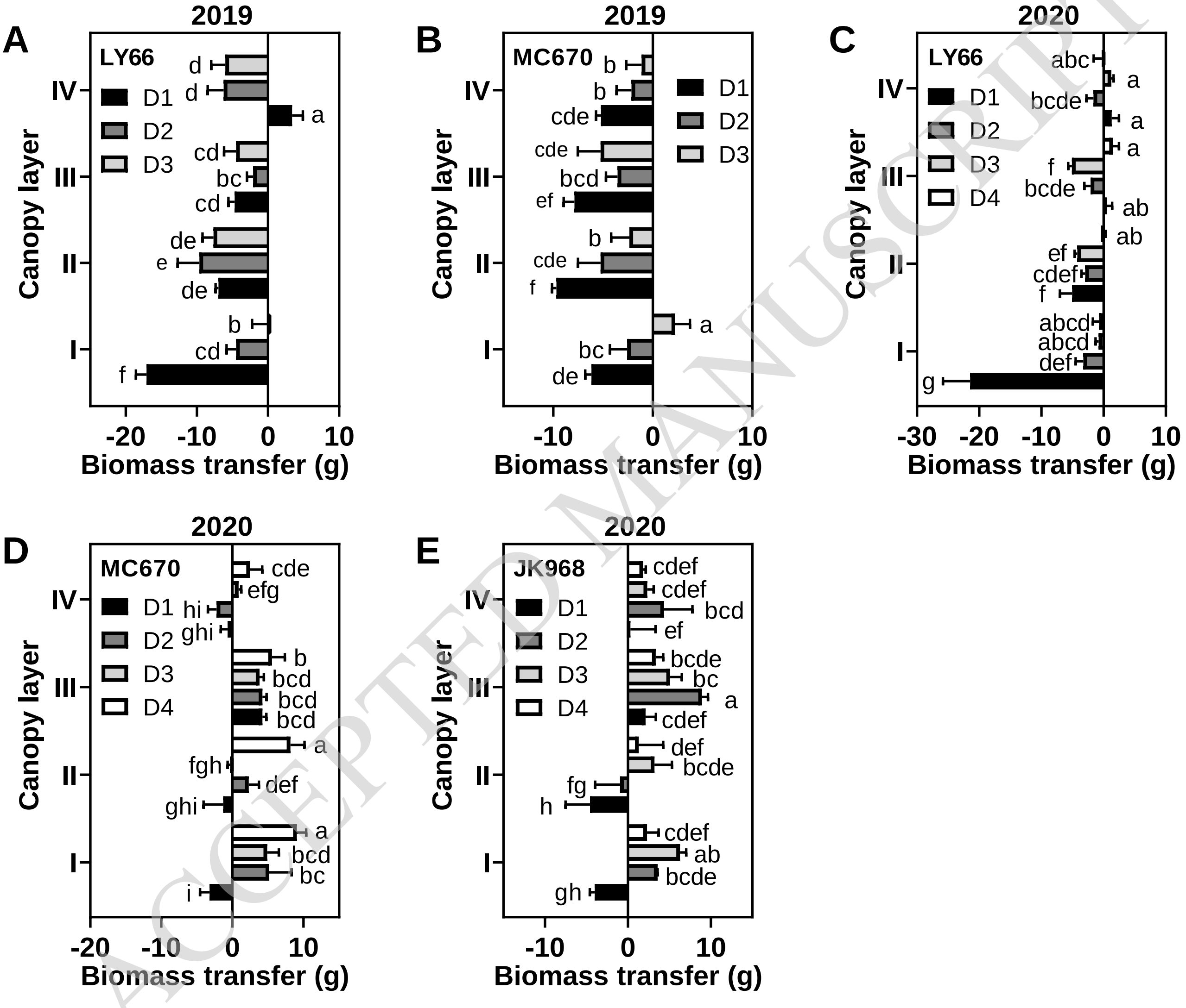
A
2019
LY66
D1
D2
D3
d
d
a
cd
bc
cd
de
e
de
b
cd
f
IV
III
II
I
Canopy layer
-20
-10
0
10
Biomass transfer (g)
B
2019
MC670
D1
D2
D3
b
b
cde
cde
bcd
ef
b
cde
f
a
bc
de
IV
III
II
I
Canopy layer
-10
0
10
Biomass transfer (g)
C
2020
LY66
D1
D2
D3
D4
abc
a
bcde
a
a
f
bcde
ab
ab
ef
cdef
f
abcd
abcd
def
g
IV
III
II
I
Canopy layer
-30
-20
-10
0
10
Biomass transfer (g)
D
2020
MC670
D1
D2
D3
D4
cde
efg
hi
ghi
b
bcd
bcd
bcd
a
fgh
def
ghi
a
bcd
bc
i
IV
III
II
I
Canopy layer
-20
-10
0
10
Biomass transfer (g)
E
2020
JK968
D1
D2
D3
D4
cdef
cdef
bcd
ef
bcde
bc
a
cdef
def
bcde
fg
h
cdef
ab
bcde
gh
IV
III
II
I
Canopy layer
-10
0
10
Biomass transfer (g)

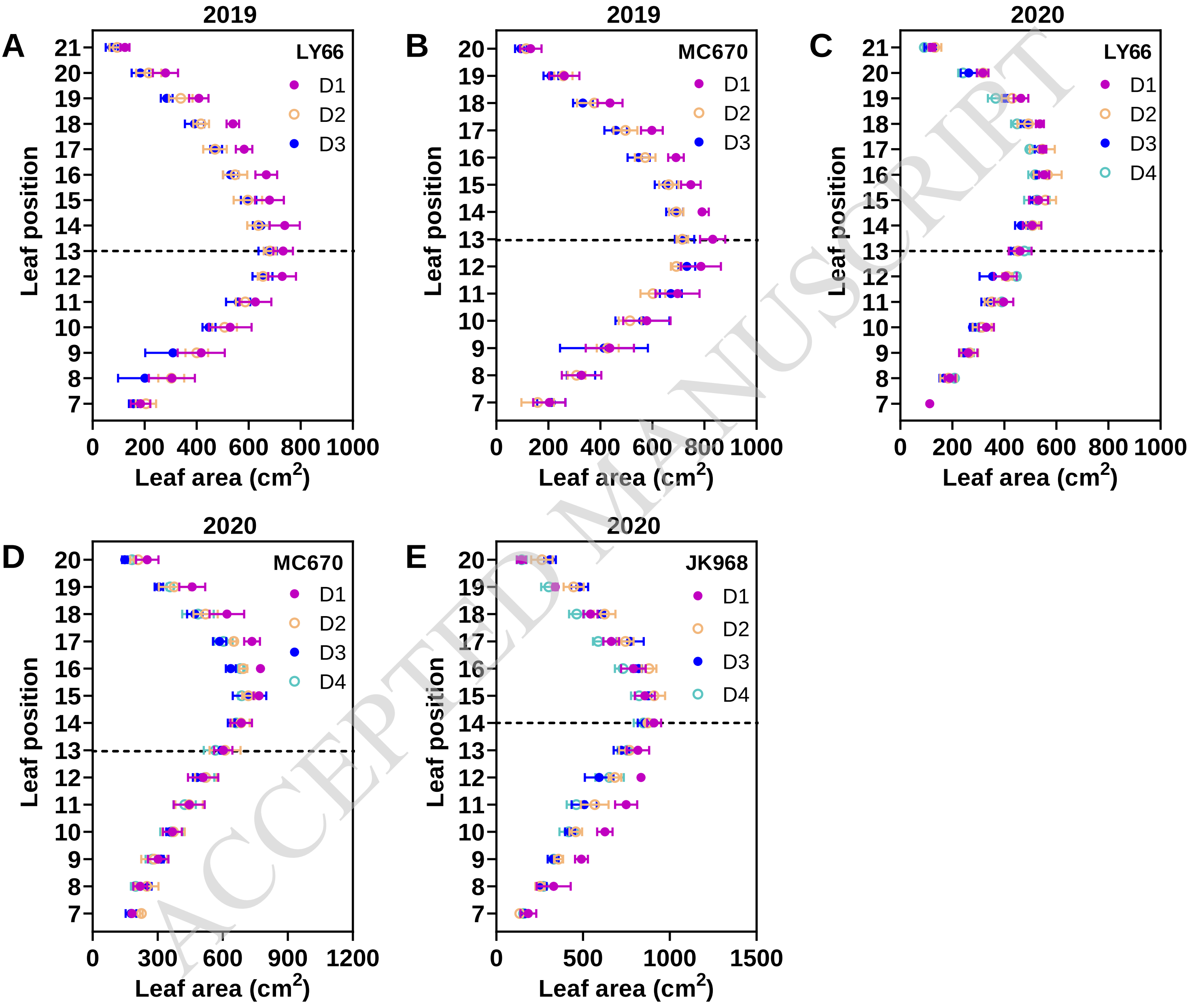
2019
A
LY66
D1
D2
D3
Leaf position
21
20
19
18
17
16
15
14
13
12
11
10
9
8
7
0
200
400
600
800
1000
Leaf area (cm^2)
2019
B
MC670
D1
D2
D3
Leaf position
20
19
18
17
16
15
14
13
12
11
10
9
8
7
0
200
400
600
800
1000
Leaf area (cm^2)
2020
C
LY66
D1
D2
D3
D4
Leaf position
21
20
19
18
17
16
15
14
13
12
11
10
9
8
7
0
200
400
600
800
1000
Leaf area (cm^2)
2020
D
MC670
D1
D2
D3
D4
Leaf position
20
19
18
17
16
15
14
13
12
11
10
9
8
7
0
300
600
900
1200
Leaf area (cm^2)
2020
E
JK968
D1
D2
D3
D4
Leaf position
20
19
18
17
16
15
14
13
12
11
10
9
8
7
0
500
1000
1500
Leaf area (cm^2)

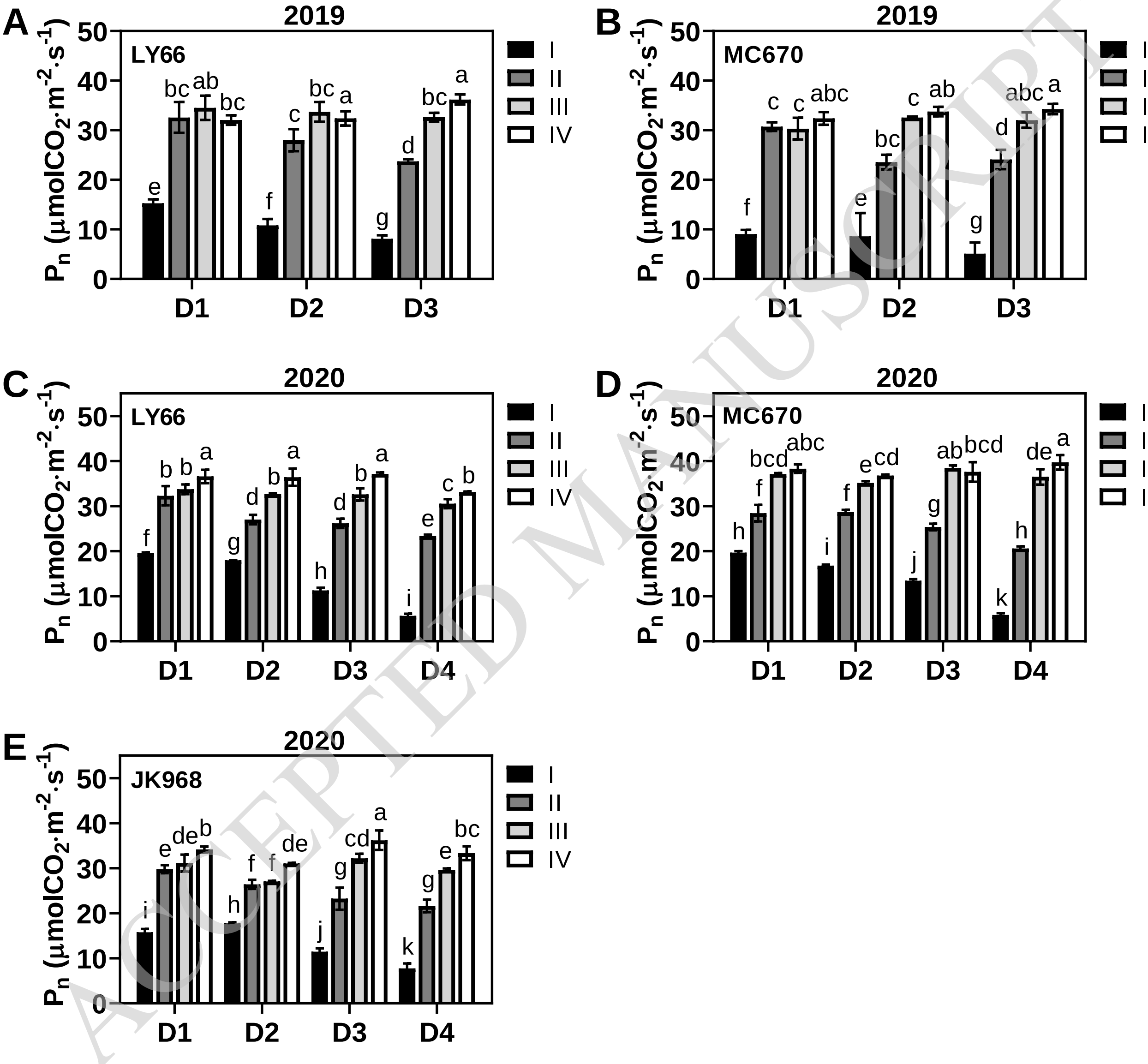
A
2019
LY66
B
2019
MC670
C
2020
LY66
D
2020
MC670
E
2020
JK968
P_n (μmolCO$_2$·m^{-2}·s^{-1})
0
10
20
30
40
50
D1
D2
D3
D4
I
II
III
IV
A: D1 e, bc, ab, bc; D2 f, c, bc, a; D3 g, d, bc, a
B: D1 f, c, c, abc; D2 e, bc, c, ab; D3 g, d, abc, a
C: D1 f, b, b, a; D2 g, d, b, a; D3 h, d, b, a; D4 i, e, c, b
D: D1 h, f, bcd, abc; D2 i, f, e, cd; D3 j, g, ab, bcd; D4 k, h, de, a
E: D1 i, e, de, b; D2 h, f, f, de; D3 j, g, cd, a; D4 k, g, e, bc

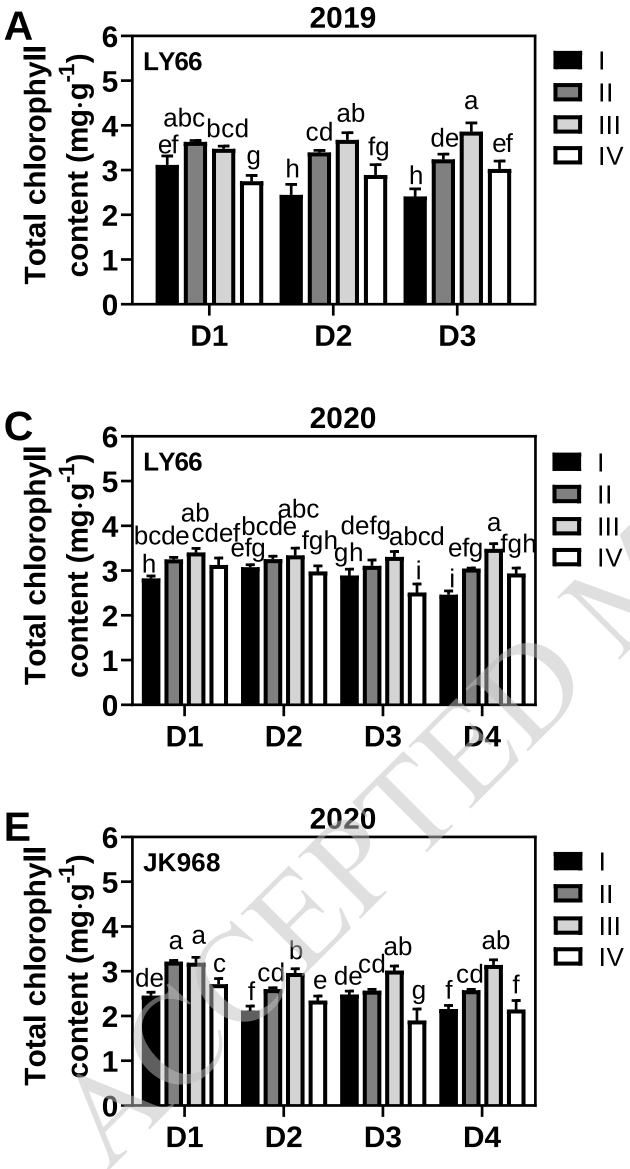
A
2019
LY66
Total chlorophyll content ($mg \cdot g^{-1}$)
0
1
2
3
4
5
6
ef
abc
bcd
g
h
cd
ab
fg
h
de
a
ef
D1
D2
D3
■ I
■ II
■ III
□ IV
B
2019
MC670
d
a
a
d
e
b
a
d
e
c
a
d
C
2020
LY66
h
bcde
ab
cdef
efg
bcde
abc
fgh
gh
defg
abcd
i
i
efg
a
fgh
D4
D
2020
MC670
bc
ab
ab
e
bc
ab
ab
f
d
cd
a
f
e
cd
ab
e
E
2020
JK968
de
a
a
c
f
cd
b
e
de
cd
ab
g
f
cd
ab
f

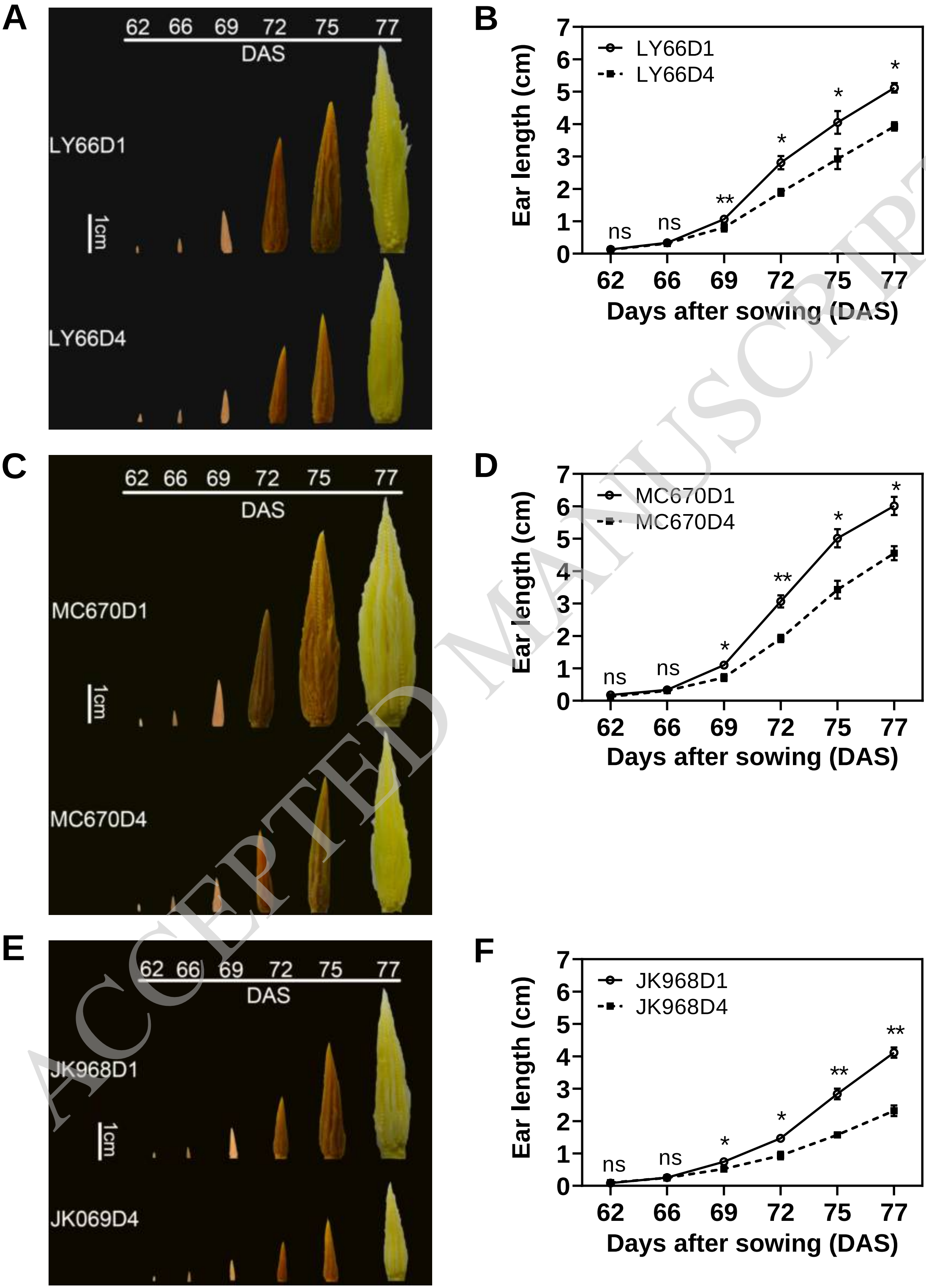
A
62 66 69 72 75 77
DAS
LY66D1
1cm
LY66D4
B
LY66D1
LY66D4
Ear length (cm)
0 1 2 3 4 5 6 7
ns ns ** * * *
62 66 69 72 75 77
Days after sowing (DAS)
C
62 66 69 72 75 77
DAS
MC670D1
1cm
MC670D4
D
MC670D1
MC670D4
Ear length (cm)
0 1 2 3 4 5 6 7
ns ns * ** * *
62 66 69 72 75 77
Days after sowing (DAS)
E
62 66 69 72 75 77
DAS
JK968D1
1cm
JK069D4
F
JK968D1
JK968D4
Ear length (cm)
0 1 2 3 4 5 6 7
ns ns * * ** **
62 66 69 72 75 77
Days after sowing (DAS)

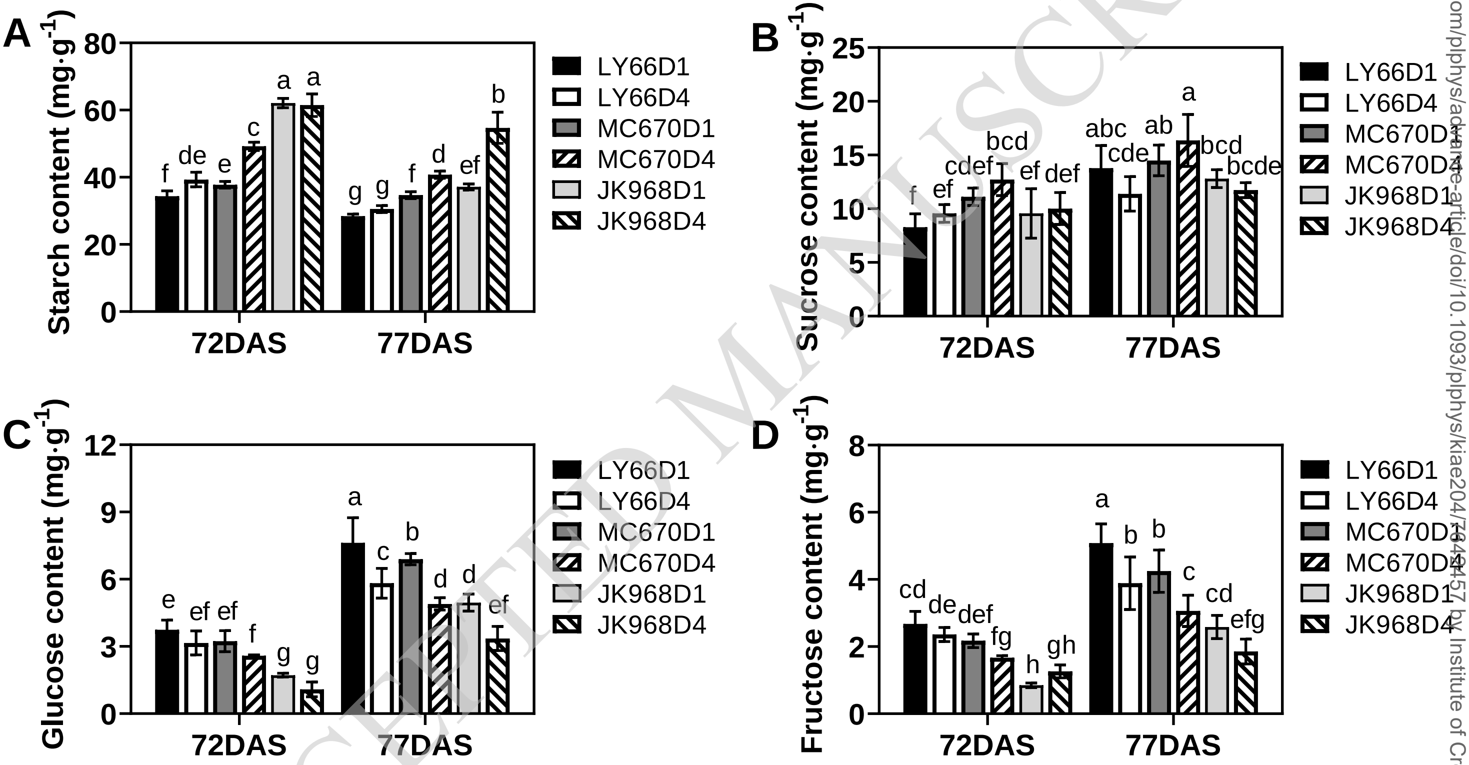
A
Starch content (mg·g-1)
0
20
40
60
80
f
de
e
c
a
a
g
g
f
d
ef
b
72DAS
77DAS
LY66D1
LY66D4
MC670D1
MC670D4
JK968D1
JK968D4
B
Sucrose content (mg·g-1)
0
5
10
15
20
25
f
ef
cdef
bcd
ef
def
abc
cde
ab
a
bcd
bcde
72DAS
77DAS
LY66D1
LY66D4
MC670D1
MC670D4
JK968D1
JK968D4
C
Glucose content (mg·g-1)
0
3
6
9
12
e
ef
ef
f
g
g
a
c
b
d
d
ef
72DAS
77DAS
LY66D1
LY66D4
MC670D1
MC670D4
JK968D1
JK968D4
D
Fructose content (mg·g-1)
0
2
4
6
8
cd
de
def
fg
h
gh
a
b
b
c
cd
efg
72DAS
77DAS
LY66D1
LY66D4
MC670D1
MC670D4
JK968D1
JK968D4

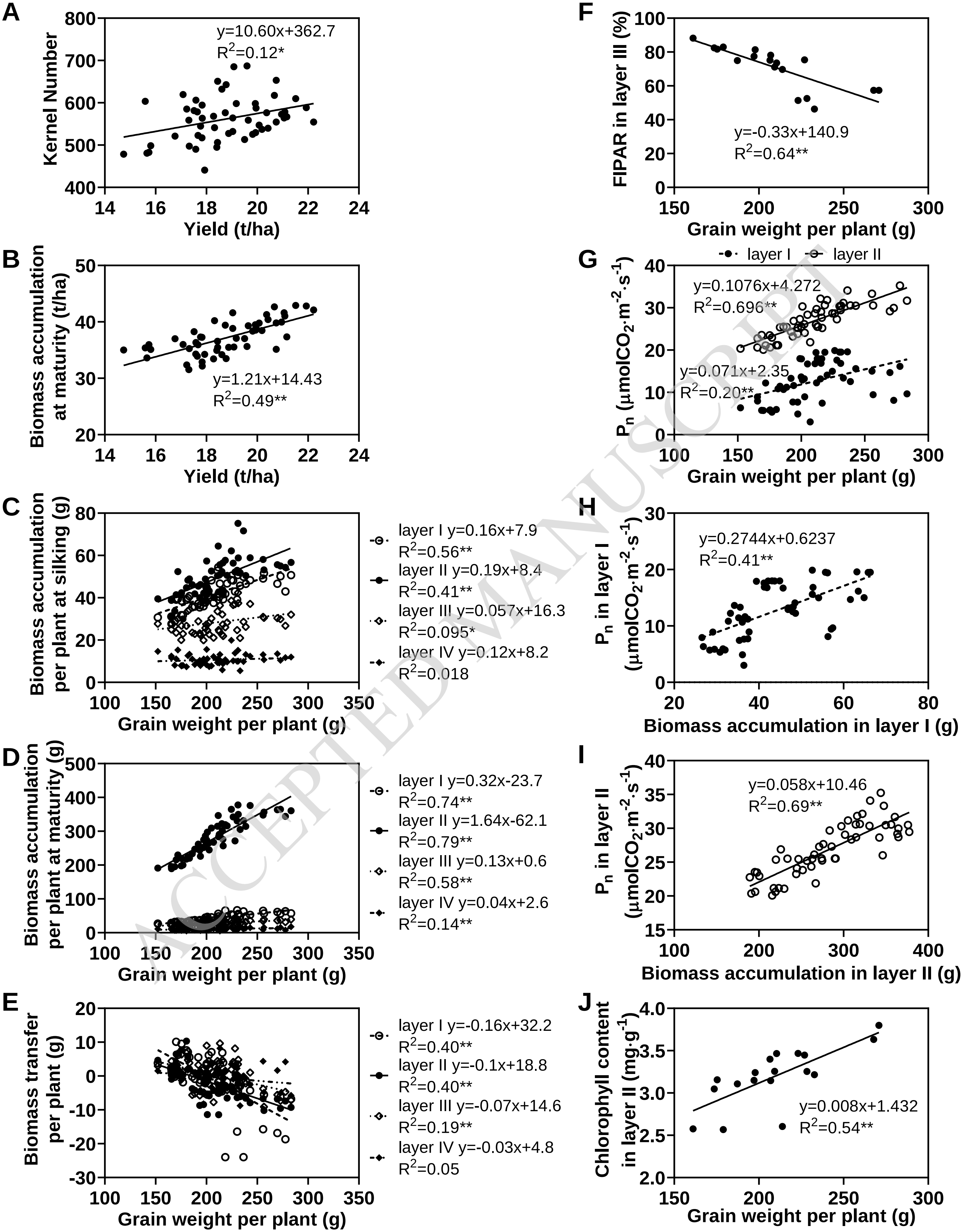
A
Kernel Number
Yield (t/ha)
y=10.60x+362.7
R^2=0.12*
B
Biomass accumulation at maturity (t/ha)
Yield (t/ha)
y=1.21x+14.43
R^2=0.49**
C
Biomass accumulation per plant at silking (g)
Grain weight per plant (g)
layer I y=0.16x+7.9
R^2=0.56**
layer II y=0.19x+8.4
R^2=0.41**
layer III y=0.057x+16.3
R^2=0.095*
layer IV y=0.12x+8.2
R^2=0.018
D
Biomass accumulation per plant at maturity (g)
Grain weight per plant (g)
layer I y=0.32x-23.7
R^2=0.74**
layer II y=1.64x-62.1
R^2=0.79**
layer III y=0.13x+0.6
R^2=0.58**
layer IV y=0.04x+2.6
R^2=0.14**
E
Biomass transfer per plant (g)
Grain weight per plant (g)
layer I y=-0.16x+32.2
R^2=0.40**
layer II y=-0.1x+18.8
R^2=0.40**
layer III y=-0.07x+14.6
R^2=0.19**
layer IV y=-0.03x+4.8
R^2=0.05
F
FIPAR in layer III (%)
Grain weight per plant (g)
y=-0.33x+140.9
R^2=0.64**
G
layer I
layer II
P_n (μmolCO$_2\cdot$m$^{-2}\cdot$s^{-1})
Grain weight per plant (g)
y=0.1076x+4.272
R^2=0.696**
y=0.071x+2.35
R^2=0.20**
H
P_n in layer I (μmolCO$_2\cdot$m$^{-2}\cdot$s^{-1})
Biomass accumulation in layer I (g)
y=0.2744x+0.6237
R^2=0.41**
I
P_n in layer II (μmolCO$_2\cdot$m$^{-2}\cdot$s^{-1})
Biomass accumulation in layer II (g)
y=0.058x+10.46
R^2=0.69**
J
Chlorophyll content in layer II (mg$\cdot$g^{-1})
Grain weight per plant (g)
y=0.008x+1.432
R^2=0.54**

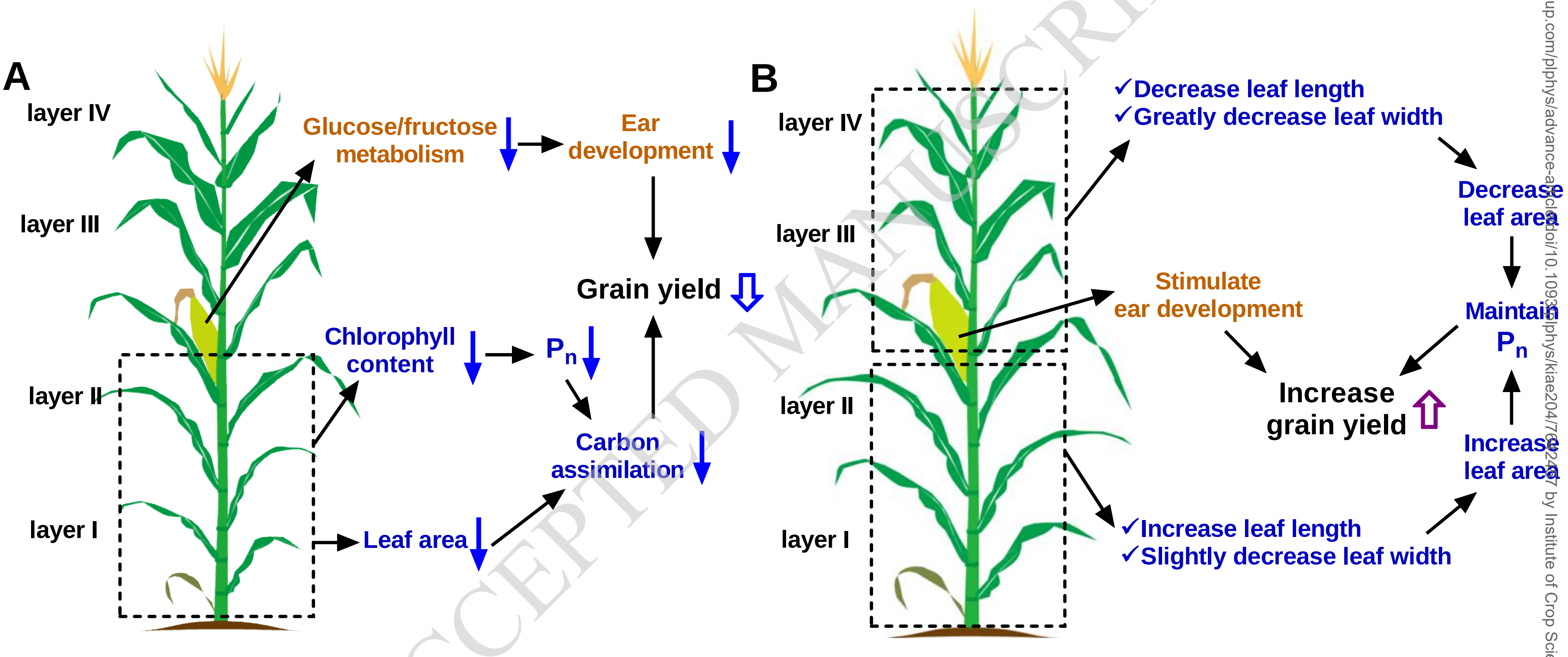
A
layer IV
layer III
layer II
layer I
Glucose/fructose metabolism
Ear development
Grain yield
Chlorophyll content
P_n
Carbon assimilation
Leaf area
B
layer IV
layer III
layer II
layer I
✓Decrease leaf length
✓Greatly decrease leaf width
Decrease leaf area
Stimulate ear development
Maintain P_n
Increase grain yield
Increase leaf area
✓Increase leaf length
✓Slightly decrease leaf width

Parsed Citations

Allison JCS, Watson DJ (1966) The production and distribution of dry matter in maize after flowering. Ann Bot 30: 365-381.
Google Scholar: Author Only Title Only Author and Title

Andrade FH, Vega C, Uhart S, Cirilo A, Cantarero M, Valentinuz O (1999) Kernel number determination in maize. Crop Sci 39(2): 453-459.
Google Scholar: Author Only Title Only Author and Title

Andrea S, Di BD, Pierangelo B, Olga G, Giorgio M (2016) Investigating the European beech (Fagus sylvatica L.) leaf characteristics along the vertical canopy profile: leaf structure, photosynthetic capacity, light energy dissipation and photoprotection mechanisms. Tree Physiol 36(9): 1060-1076.
Google Scholar: Author Only Title Only Author and Title

Assefa Y, Carter P, Hinds M, Bhalla G, Schon R, Jeschke M, Paszkiewicz S, Smith S, Ciampitti IA (2018) Analysis of long term study indicates both agronomic optimal plant density and increase maize yield per plant contributed to yield gain. Sci Rep 8: 4937.
Google Scholar: Author Only Title Only Author and Title

Cárcova J, Uribelarrea M, Borrás L, Otegui ME, Westgate ME (2000) Synchronous pollination within and between ears improves kernel set in maize. Crop Sci 40(4): 1056-1061.
Google Scholar: Author Only Title Only Author and Title

Chen W, Zhang J, Deng X (2019) The spike weight contribution of the photosynthetic area above the upper internode in a winter wheat under different N and mulching regimes. Crop J 7: 89-100.
Google Scholar: Author Only Title Only Author and Title

Chen Y, Wu D, Mu X, Xiao C, Chen F, Yuan L, Mi G (2015) Vertical distribution of photosynthetic nitrogen use efficiency and its response to nitrogen in field-grown maize. Crop Sci 56: 397-407.
Google Scholar: Author Only Title Only Author and Title

Ciampitti IA, Vyn TJ (2013) Grain nitrogen source changes over time in maize: a review. Crop Sci 53: 366-377.
Google Scholar: Author Only Title Only Author and Title

Collison RF, Raven EC, Pignon CP, Long SP (2020) Light, not age, underlies the maladaptation of maize and miscanthus photosynthesis to self-shading. Front Plant Sci 11: 783.
Google Scholar: Author Only Title Only Author and Title

Cui H, Camberato JJ, Jin L, Zhang J (2015) Effects of shading on spike differentiation and grain yield formation of summer maize in the field. Int J Biometeorol 59: 1189-1200.
Google Scholar: Author Only Title Only Author and Title

Deng J, Ran J, Wang Z, Fan Z, Wang G, Ji M, Liu J, Wang Y, Liu J, Brown JH (2012) Models and tests of optimal density and maximal yield for crop plants. Proc Natl Acad Sci U S A 109: 15823-15828.
Google Scholar: Author Only Title Only Author and Title

Duan F, Wei Z, Soualiou S, Zhou W (2023) Nitrogen partitioning in maize organs and underlined mechanisms from different plant density levels and N application rate in China. Field Crops Res 294: 108874.
Google Scholar: Author Only Title Only Author and Title

Escobar-Gutiérrez AJ, Combe L (2012) Senescence in field-grown maize: from flowering to harvest. Field Crops Res 134: 47-58.
Google Scholar: Author Only Title Only Author and Title

FAO (2021) Statistics for trade of crops and livestock products-dataset. https://www.fao.org/faostat/en/#data/QCL.
Google Scholar: Author Only Title Only Author and Title

Gaju O, DeSilva J, Carvalho P, Hawkesford MJ, Griffiths S, Greenland A, Foulkes MJ (2016) Leaf photosynthesis and associations with grain yield, biomass and nitrogen-use efficiency in landraces, synthetic-derived lines and cultivars in wheat. Field Crops Res 193: 1-15.
Google Scholar: Author Only Title Only Author and Title

Guo Y, Yin W, Fan H, Fan Z, Hu F, Yu A, Zhao C, Chai Q, Aziiba EA, Zhang X (2021) Photosynthetic physiological characteristics of water and nitrogen coupling for enhanced high-density tolerance and increased yield of maize in arid irrigation regions. Front Plant Sci 12: 726568.
Google Scholar: Author Only Title Only Author and Title

Gustin JL, Boehlein SK, Shaw JR, Junior W, Settles AM, Webster A (2018) Ovary abortion is prevalent in diverse maize inbred lines and is under genetic control. Sci Rep 8: 13032.
Google Scholar: Author Only Title Only Author and Title

Hans-Wilhelm N, Claudio S, Anne O (2018) Metabolic gene clusters in eukaryotes. Annu Rev Genet 52(1): 159-183.

Google Scholar: Author Only Title Only Author and Title

Hikosaka K, Anten NP, Borjigidai A, Kamiyama C, Sakai H, Hasegawa T, Oikawa S, Iio A, Watanabe M, Koike T, Nishina K, Ito A (2016) A meta-analysis of leaf nitrogen distribution within plant canopies. Ann Bot 118: 239-247.
Google Scholar: Author Only Title Only Author and Title

Hu J, Ren B, Dong S, Liu P, Zhao B, Zhang J (2022) Poor development of spike differentiation triggered by lower photosynthesis and carbon partitioning reduces summer maize yield after waterlogging. Crop J 10(2): 478-489.
Google Scholar: Author Only Title Only Author and Title

Hu W, Lu Z, Meng F, Li X, Cong R, Ren T, Sharkey TD, Lu J (2020) The reduction in leaf area precedes that in photosynthesis under potassium deficiency: the importance of leaf anatomy. New Phytol 227: 1749-1763.
Google Scholar: Author Only Title Only Author and Title

Li Y, Song H, Zhou L, Xu Z, Zhou G (2019) Vertical distributions of chlorophyll and nitrogen and their associations with photosynthesis under drought and rewatering regimes in a maize field. Agr Forest Meteorol 272-273: 40-54.
Google Scholar: Author Only Title Only Author and Title

Lichtenthaler H (1987) Chlorolphylls and carotenoids: pigments of photosynthetic biomembranes. Method Enzymol 148: 350-382.
Google Scholar: Author Only Title Only Author and Title

Liu G, Yang Y, Guo X, Liu W, Xie R, Ming B, Xue J, Wang K, Li S, Hou P (2023) A global analysis of dry matter accumulation and allocation for maize yield breakthrough from 1.0 to 25.0 Mg ha-1. Resour Conserv Recy 188: 106656.
Google Scholar: Author Only Title Only Author and Title

Luo N, Meng Q, Feng P, Qu Z, Yu Y, Liu D, Müller C, Wang P (2023) China can be self-sufficient in maize production by 2030 with optimal crop management. Nat Commun 14: 2637.
Google Scholar: Author Only Title Only Author and Title

Ma L, Li Y, Wu P, Zhao X, Gao X, Chen X (2020) Recovery growth and water use of intercropped maize following wheat harvest in wheat/maize relay strip intercropping. Field Crops Res 256: 107924.
Google Scholar: Author Only Title Only Author and Title

Macneill GJ, Sahar M, Minow MAA, Patterson JA, Tetlow IJ, Emes MJ (2017) Starch as a source, starch as a sink: the bifunctional role of starch in carbon allocation. J Exp Bot 68(16): 4433-4453.
Google Scholar: Author Only Title Only Author and Title

Mastrodomenico AT, Haegele JW, Seebauer JR, Below F (2018) Yield stability differs in commercial maize hybrids in response to changes in plant density, nitrogen fertility, and environment. Crop Sci 58(1): 230-241.
Google Scholar: Author Only Title Only Author and Title

Odorico PD, Emmel C, Revill A, Liebisch F, Eugster W, Buchmann N (2019) Vertical patterns of photosynthesis and related leaf traits in two contrasting agricultural crops. Funct Plant Biol 46(3): 213-227.
Google Scholar: Author Only Title Only Author and Title

Otegui ME, Bonhomme R (1998) Grain yield components in maize: I. Ear growth and kernel set. Field Crops Res 56(3): 247-256.
Google Scholar: Author Only Title Only Author and Title

Pagano E, Cela S, Maddonni GA, Otegui ME (2007) Intraspecific competition in maize: Ear development, flowering dynamics and kernel set of early-established plant hierarchies. Field Crops Res 102: 198-209.
Google Scholar: Author Only Title Only Author and Title

Parvathaneni RK, Bertolini E, Shamimuzzaman M, Vera DL, Lung PY, Rice BR, Zhang J, Brown PJ, Lipka AE, Bass HW, Eveland AL (2020) The regulatory landscape of early maize inflorescence development. Genome Biol 21(1): 165.
Google Scholar: Author Only Title Only Author and Title

Pawar R, Rana VS (2019) Manipulation of source-sink relationship in pertinence to better fruit quality and yield in fruit crops: A review. Agric Rev 40(3): 200-207.
Google Scholar: Author Only Title Only Author and Title

Perez R, Fournier C, Cabrera-Bosquet L, Artzet S, Tardieu F (2019) Changes in the vertical distribution of leaf area enhanced light interception efficiency in maize over generations of selection. Plant Cell Environ 42(7): 2105-2119.
Google Scholar: Author Only Title Only Author and Title

Prajal P, Günther F, Harrij W, Reusser DE, Kropp JP, Luis GAJ. (2015). Closing yield gaps: How sustainable can we be? PLoS One 10(5): e0129487.
Google Scholar: Author Only Title Only Author and Title

Raza MA, Bin Khalid MH, Zhang X, Feng LY, Khan I, Hassan MJ, Ahmed M, Ansar M, Chen YK, Fan YF, Yang F, Yang W (2019) Effect of planting patterns on yield, nutrient accumulation and distribution in maize and soybean under relay intercropping systems. Sci Rep 9(1): 4947.

Google Scholar: Author Only Title Only Author and Title

Rossini MA, Maddonni GA, Otegui ME (2011) Inter-plant competition for resources in maize crops grown under contrasting nitrogen supply and density: Variability in plant and ear growth. Field Crops Res 121(3): 373-380.
Google Scholar: Author Only Title Only Author and Title

Ruben V, Omar VD, Susan M, Fadia C, Kefauver SC, Jordi B, Dolores SM, Nieves A, Luis AJ (2018) Durum wheat ears perform better than the flag leaves under water stress: Gene expression and physiological evidence. Environ Exp Bot 153: 271-285.
Google Scholar: Author Only Title Only Author and Title

Sarlikioti V, de Visser PH, Buck-Sorlin GH, Marcelis LF (2011) How plant architecture affects light absorption and photosynthesis in tomato: towards an ideotype for plant architecture using a functional-structural plant model. Ann Bot 108(6):1065-1073.
Google Scholar: Author Only Title Only Author and Title

Shao D, Villet O, Zhang Z, Choi SW, Yan J, Ritterhoff J, Gu HW, Djukovic D, Christodoulou D, Kolwicz Jr S, Raftery D, Tian R (2018) Glucose promotes cell growth by suppressing branched-chain amino acid degradation. Nat Commun 9: 2935.
Google Scholar: Author Only Title Only Author and Title

Sher A, Khan A, Li JC, Ahmad MI, Jamoro SA (2017) Response of maize grown under high plant density; performance, issues and management - A critical review. Adv Crop Sci Tech 5: 275.
Google Scholar: Author Only Title Only Author and Title

Simkin AJ, Lopez-Calcagno PE, Raines CA (2019) Feeding the world: improving photosynthetic efficiency for sustainable crop production. J Exp Bot 70: 1119-1140.
Google Scholar: Author Only Title Only Author and Title

Slattery RA, Walker BJ, Weber APM, Ort DR (2018) The impacts of fluctuating light on crop performance. Plant Physiol 176(2): 990-1003.
Google Scholar: Author Only Title Only Author and Title

Song H, Li Y, Zhou L, Xu Z, Zhou G (2018) Maize leaf functional responses to drought episode and rewatering. Agric For Meteorol 249: 57-70.
Google Scholar: Author Only Title Only Author and Title

Sultana F, Dev W, Xin M, Han Y, Feng L, Lei Y, Yang B, Wang G, Li X, Wang Z, Xing F, Xiong S, Li Y (2023) Competition for light interception in different plant canopy characteristics of diverse cotton cultivars. Genes (Basel) 14(2):364.
Google Scholar: Author Only Title Only Author and Title

Tian X, Engel BA, Qian H, Hua E, Sun S, Wang Y (2021) Will reaching the maximum achievable yield potential meet future global food demand? J Clean Prod 294: 1-12.
Google Scholar: Author Only Title Only Author and Title

Timlin DJ, Fleisher DH, Kemanian AR, Reddy VR (2014) Plant density and leaf area index effects on the distribution of light transmittance to the soil surface in maize. Agron J 106(5): 1828-1837.
Google Scholar: Author Only Title Only Author and Title

Uribelarrea M, Cárcova J, Borrás L, Otegui ME (2008) Enhanced kernel set promoted by synchronous pollination determines a tradeoff between kernel number and kernel weight in temperate maize hybrids. Field Crops Res 105:172-181.
Google Scholar: Author Only Title Only Author and Title

Valluru R (2015) Fructan and hormone connections. Front Plant Sci 6: 180.
Google Scholar: Author Only Title Only Author and Title

Wang F, Xie R, Ming B, Wang K, Hou P, Chen J, Liu G, Zhang G, Xue J, Li S (2021) Dry matter accumulation after silking and kernel weight are the key factors for increasing maize yield and water use efficiency. Agric Water Manag 254: 106938.
Google Scholar: Author Only Title Only Author and Title

Wei H, Kong D, Yang J, Wang H (2020) Light regulation of stomata development and patterning: shifting the paradigm from Arabidopsis to grasses. Plant Commun 1(2): 9.
Google Scholar: Author Only Title Only Author and Title

Wilson JH, Allison JCS (1978) Effect of plant population on ear differentiation and growth in maize. Ann Appl Biol 90: 127-132.
Google Scholar: Author Only Title Only Author and Title

Xin Q, Zhang L, Qu Y, Geng H, Li X, Peng S (2023) Satellite mapping of maize cropland in one-season planting areas of China. Sci Data 10: 437.
Google Scholar: Author Only Title Only Author and Title

Xu Z, Zhou G, He Q (2021) Vertical distribution of gas exchanges and their integration throughout the entire canopy in a maize field. Photosyn Res 147(3): 269-281.
Google Scholar: Author Only Title Only Author and Title

Yan Y, Hou P, Duan FY, Niu L, Dai T, Wang K, Zhao M, Li S, Zhou W (2021) Improving photosynthesis to increase grain yield potential: an analysis of maize hybrids released in different years in China. Photosyn Res 150: 295-311.
Google Scholar: Author Only Title Only Author and Title

Zhang D, Sun Z, Feng L, Bai W, Zhang L (2020) Maize plant density affects yield, growth and source-sink relationship of crops in maize/peanut intercropping. Field Crops Res 257: 107926.
Google Scholar: Author Only Title Only Author and Title

Zhang J, Peng Z, Li T (2009) Effects of different N application rates on the dynamic accumulation and distribution of assimilate and N content in maize. Journal of Hebei Agricuture University 2: 1-5 (in Chinese with English abstract).
Google Scholar: Author Only Title Only Author and Title

Zhang M, Chen T, Hojatollah L (2018) How plant density affects maize spike differentiation, kernel set, and grain yield formation in northeast China? J Integr Agric 17: 53-65.
Google Scholar: Author Only Title Only Author and Title

Zhang P, Xia L, Sun Z, Zhang T (2023) Analysis of spatial and temporal changes and driving forces of arable land in the Weibei dry plateau region in China. Sci Rep 13: 20618.
Google Scholar: Author Only Title Only Author and Title

Zhang Y, Wang R, Wang S, Ning F, Li J (2019) Effect of planting density on deep soil water and maize yield on the Loess Plateau of China. Agric Water Manag 223: 105655.
Google Scholar: Author Only Title Only Author and Title

Zhao J, Yang X, Lin X, Sassenrath GF, Dai S, Lv S, Chen X, Chen F, Mi G (2015) Radiation interception and use efficiency contributes to higher yields of newer maize hybrids in northeast China. Agron J 107(4): 1473-1480.
Google Scholar: Author Only Title Only Author and Title

Zheng M, Chen J, Shi Y, Li Y, Yin Y, Yang D, Luo Y, Pang D, Xu X, Li W, Ni J, Wang Y, Wang Z, Li Y (2017) Manipulation of lignin metabolism by plant densities and its relationship with lodging resistance in wheat. Sci Rep 7: 41805.
Google Scholar: Author Only Title Only Author and Title